DETERMINATION OF SHIELDING EFFECTIVENESS OF SOME SELECTED MATERIALS AVAILABLE IN LESOTHO USING MCNP CODE

This thesis submitted to the

UNIVERSITY OF GHANA

By

MOJALEFA DANIEL SELLO

(10644406)

BSc (National University of Lesotho (NUL), Lesotho), 2017

In partial fulfilment of the requirement for the award of

MASTER OF PHILOSOPHY DEGREE (MPhil)

IN

NUCLEAR SCIENCE AND TECHNOLOGY

NOVEMBER, 2019

DECLARATION

This work is the result of research undertaken by Mojalefa Daniel Sello of Department of Medical Physics of the School Nuclear and Allied sciences University of Ghana Legon of under the supervision of Professor Cyril Schandorf and Dr Philip Deatanyah in exception of references.

Sign……. Date…….

(Mojalefa Daniel Sello)

Student

Sign……. Date……..

(Dr. Philip Deatanyah)

Principal Supervisor

Sign…….. Date…….

(Prof. Cyril Schandorf)

Co-supervisor

ABSTRACT

In this study, the Monte Carlo N-particle simulation code MCNPX-2.6.0 was used to determine the shielding effectiveness of clay, wood and sandstone. This was done by determining the transmission of ^{60}Co gamma and X-rays with energies 60 keV, 120 keV and 300 keV through wood, clay and sandstone. The transport computations were done for slab shield, computing half-value layers (HVLs), tenth-value layers (TVLs), buildup factors, and attenuation coefficients (both linear and mass attenuation coefficients). Plaque, point and cylindrical source geometries were considered. The materials of thickness ranging from 0 to 50 cm with an increment of 5 cm were irradiated by each source geometry. The transmitted photon flux ranges from 69.4 % for wood down to 14.3 % while from 48.3 % down to 0.65 % and 46.8 % down to 0.48 % for clay and sandstone respectively. Wood buildup factors for ^{60}Co were found to be lower (1.28 to 2.5) compared to (2.2 to 9.84) for both clay and sandstone. The associated linear attenuation coefficients (LACs) were within 3.8E10-02 to 9.5E-02 cm^{-1} for the three materials. Similarly, for x-ray sources. The effectiveness of the three materials, comparing with the results of lead, performing cost-benefit analysis using average prices in Lesotho based on thicknesses was very economical. The transmission of x-rays ranges from 76 % for wood down to 6 % for higher energy x-rays (300 keV), from 69 % down to 1 % for 120 keV and from 65 % down to 0.5 % for 60 keV. For clay and sandstone, the transmission ranges from within 87- 89 % down to ≈ 0 % for 300 keV, 79-80 % also down to ≈ 0 % for 120 keV and 61- 63 % down to ≈ 0 % for 60 keV. For lower energy x-rays, the computed buildup factors ranged from 1.20 to 34 for the three materials whiles from 1.16 to 25 for higher energy x-rays. The

associated LACs for lower energy (9.12E-2) to higher energy x-rays (5.57E-02 cm^{-1}) for wood whiles the results for clay and sandstone were within the range 5.4E-01 to 5.7E-01 cm^{-1}. The cost-benefit analysis done on three materials using assumed monetary values (based on average prices in Lesotho) controlled by the thickness and volume of the materials for same area of 81 m^2 (9 m x 9 m), indicated the positive benefit B for three materials; $4,395 for wood with 0.91 m thickness and 73.71 m^3volume, $3,730.8 for clay with 0.46 m thickness and 34.83 m^3 volume and $4,233 for sandstone with thickness of 0.43 and 37.26 m^3 volume with the benefit based replacement of lead with assumed cost of $10,000.

DEDICATION

This work is dedicated to my country Lesotho, my parents Mr. and Mrs. Sello and my sisters (especially my Late sister Mapitso Sello who passed away while I was doing this work) and my grandmother Lekhula.

ACKNOWLEDGEMENTS

Swords, soldiers and armours are prepared for the battle but without God victory is not worth considering, hence I would like to thank God for his protection, wisdom, strength to carry on and his guidance throughout this study up to its successful completion.

Great thanks are directed to my supervisory team, I am grateful to Dr. Philip Deatanyah and Prof. Cyril Schandorf for their overwhelming support, encouragement, advices, ideas, detailed corrections and important comments which made this work a huge success.

I would also like to appreciate the support from Head of Department of Nuclear Safety and Security Dr. David Okoh Kpeglo and the entire staff of the stated department with their useful comments which made this work more successful.

Special thanks to the entire staff of the School of Nuclear and Allied Sciences and my colleagues and friends for their support.

My heartfelt appreciation goes to the Developers of the Monte Carlo N-Particle transport (MCNP) code and, without the code the work would have been more challenging.

Finally, I would like to thank my family; Mrs'Majoane Sello my mother, Mr Tohlang Sello my father, Mrs. 'Malebohang Lekhula, my Aunties and my siblings for their prayers, encouragement and support.

TABLE OF CONTENTS

LIST OF ABBREVIATIONS

HVL	Half Value Layer
TVL	Tenth Value Layer
Sv	Sieverts
MCNP	Monte Carlo N-Particle code
IAEA	International Atomic energy Agency
ICRP	International Commission on Radiological Protection
mSv	milli-Sieverts
keV	kilo-electronvolt
NCRP	National Council on Radiation Protection and measurements
CBA	Cost-Benefit Analysis
MBq	Megabecquerel
LAC	Linear Attenuation Coefficient
MAC	Mass Attenuation Coefficient
CSEWG	Cross-Section Evaluation Working Group
ENDF	Evaluated Nuclear Data File
MFP	Mean Free Path
ALARA	As Low As Reasonably Achievable

LIST OF FIGURES

LIST OF TABLES

CHAPTER ONE

INTRODUCTION

This chapter focuses on the background, problem statement, objectives, justification and scope and limitation of the research.

1.1 BACKGROUND

Radiation is used in a variety of areas such as medicine, power production, food industries and many more. X-rays were first discovered by Wilhelm Conrad Roentgen 1895. Radiation can be thought of as the propagation of energy in the form of energetic particles or electromagnetic waves, this motion is either in space or within matter. Scientists mostly knew about radiations from the 1890s and since then they have gained successful ability to invent a range of applications of this natural force ("US NRC: Uses of Radiation," 2014).

In medical use, there is a diversity of radioisotopes (nuclear materials) employed in monitoring, diagnosing and treating different abnormal conditions in the human body. In industries, radiation is used to produce power as it is one of the major needs of man's daily activities. In the agriculture and food industries, radiation is used for sterilization, food irradiation, check for food contamination and many more.

Despite these undoubted benefits of radiation in human life, if human beings are exposed to intense or high levels of radiation doses it can lead to hazardous conditions as it has an ability to alter human cells' structures. This is due to the form of radiation referred to as ionizing radiation. It is coherent that when the cell's structure is altered, then the normal operation of the cell is affected. These hazards can be avoided if the dose or amount of

radiation that impact a human body is at acceptable levels which body cells can withstand, that is, the damage being so little that cells are able to regenerate.

Naturally, the universe is inundated with radiations of diverse energy ranges, but the atmosphere is able to shield us (Lead Industries Association, 2016.). The main target of radiation protection is the protection of people (workers and public) exposed to radiation. Exposure to radiation also has genetic effects which can have significant effects on the future generation. All these considerations lead to well-calculated acceptable dose levels which play a vital role in radiation protection.

With the increased activities of man to convert matter into energy(Lead Industries Association, 2016.) and utilization of radioactive materials in various fields could result in exposure levels beyond regulatory control which could pose a hazard to workers, public and the environment.

In order to protect the workers and public from undue exposure to radiation dose, the shield design and integrity must be adequate.

Theoretically, all materials could be used as shielding materials if enough thickness is employed. There are various materials that are being used as shielding materials today such as, lead, gypsum, concrete, with depleted uranium (uranium recovered for nuclear reactor waste or tail of enrichment plant) recently been noticed and few other materials(Peter J. Biggs, 2014). The use of these materials is the result of experiments that have been conducted to investigate their shielding effectiveness. These well-established radiation shielding materials are not readily available to all localities thus making shielding of radiation facilities at some localities such as Lesotho costly and difficult to achieve

adequate protection. This makes it necessary to investigate and identify new and suitable radiation shielding materials which will be readily available and cost-effective in shielding such facilities.

In this present study, an attempt is made to evaluate the radiation shielding integrity and effectiveness of other shielding materials abundantly available in Lesotho using Monte Carlo code MCNP as a computational tool.

This MCNP is a general-purpose Monte Carlo n-particle code applied in transportation of neutrons, photons, electrons, or coupled neutron/photon/electron transport (Alrammah, 2016).

1.2 PROBLEM STATEMENT

Lesotho is one of the small developing countries with an area of 30 355km^2 landlocked and encircled by South Africa, its population is 2.233 million as of 2017. Lesotho is one of the countries in Africa with few radiation facilities but huge potential to increase these facilities in the near future. There are a lot of radiation facilities that are awaiting installation but cannot be started due to unavailability of adequately shielded rooms. Some of the facilities are inadequately shielded such hiptals whre x-rays are used. This is further aggravated by the absence of established shielding materials required to establish these facilities. These raw materials are not available in Lesotho. There are only X-ray generators in Lesotho and mostly are in mining industries which are used as scanners, density gauges, tracers, sorters, for medical purposes and so on, few are at some hospitals which are medical X-rays, this shows that more radiation facilities needed in the country for improved utilization of radiation not only limited to mining industries and more are needed for medical purposes in future. In future the country also is hoping to have gamma and neutron facilities and it

can be better to provide cheaper materials for shielding and other purposes. This work researched into cheaper materials available in Lesotho which can be used to adequately shield radiation facilities throughout the country.

1.3 RELEVANCE AND JUSTIFICATION

For optimum protection and safety of the workers and the public from radiation hazards, a search for suitable local materials for cost-effective shielding is required. Materials with potential for radiation shielding are available in Lesotho such as sandstone, clay and wood which need to be characterized in terms of their shielding properties. The shielding characteristics and design of the selected local materials will provide the mechanisms for cost-effective shielding of radiation facilities in Lesotho. The scientific findings shall be published in a suitable journal.

1.4 AIM

The main objective of this research is to determine and evaluate the shielding effectiveness of some selected materials found in Lesotho using the MCNP code.

1.5 The specific objectives:

1) To investigate the Radiological properties by determining the attenuation properties and transmission factors of the selected materials.
2) Use MCNP code to simulate and study the shielding effectiveness
3) To perform economic analysis on the materials using cost-benefit analysis (CBA) method
4) Make appropriate recommendations to regulatory authorities and end-user facilities from findings.

1.6 SCOPE AND LIMITATION

The research work will be limited to the following materials: sandstone, clay and wood which will be modelled to shield gamma rays and x-rays using the MCNP code. The shield design and characteristics will be limited to biological shield purposely to minimize exposure to personnel in radiation environments. The work focuses on x-rays and gamma-rays plaque, cylindrical and isotropic sources geometries considering only slab material geometry. X-ray spectrum was limited up to 300 keV divided into two intervals; (60 keV to 120 keV) and (120 keV to 300 keV) and ^{60}Co gamma source, expectation will be to find results indicating that these materials can be used as less costly but effective materials compared to materials such Lead.

1.7 ORGANIZATION OF THE THESIS

This work is composed of five chapters. Chapter one covers the backgroundof the research work, problem statement, objectives, justification, scope and limitation of the research. The second chapter focuses on the review of existing literature related to the study. The third chapter gives the materials the methods used to conduct the research work. The fourth chapter covers the results obtained, analysis and discussions on the findings. Chapter five provides an account of the conclusion and recommendations made to relevant stakeholders.

CHAPTER TWO

LITERATURE REVIEW

This chapter surveys the literature which covers the conceptual framework for shielding, characterization of shielding materials, sources of radiation exposures to be shielded against, attenuation properties of shielding materials , dosimetry, Monte Carlo methods ,advances in shielding methods, shielding materials optimization methods and cost-benefit analysis for shieling effectiveness.

2.0 CONCEPT OF RADIATION SHIELDING

Basically, shielding is placing the material between the source and a detector or an environment to be protected, the attenuation properties of a material and its thickness allow mankind to continue nuclear activities beyond the shielding without being exposed unacceptably to harmful radiation.

It is essential to understand the interaction of gamma with a matter which helps in the detection and shielding of gamma. When radiation beam enters a volume is either scattered, absorbed and or transmitted through; the processes involved are discussed under attenuation properties, the scattering and absorption are termed as attenuation. Absorption simply means that when a particle is absorbed after the collision, no other particle of exactly same nature is emitted while scattering means that after the collision, particle proceeds with either its direction or energy altered. The fundamental law of attenuation is illustrated in figure 2.1 as follows.(Nelson & Rewy, 1909)

$$I = I_0 e^{-\mu L} \ldots\ldots\ldots\ldots\ldots\ldots\ldots\ldots\ldots\ldots (1)$$

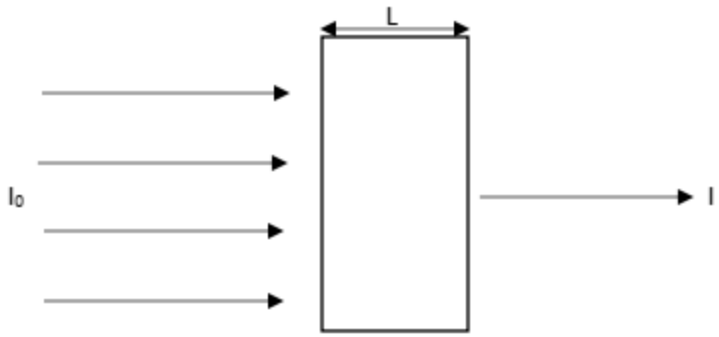

Figure 2.1 The fundamental law of attenuation of gamma, with the transmitted rays I through the thickness L of the material (Shultis & Faw, 1979).

μ is the linear attenuation coefficient of the material defined as the attenuation of radiation per unit length. It can be noted from the definition that μ has the dimensions of inverse length (1/cm).(Environmental Health and Safety's Radiation Control office, 2011).

I_o is the initial intensity and I the transmitted intensity

2.1 X-RAY, GAMMA RAY AND SOURCE CHARACTERIZATION

2.1.1 X-rays

The x-rays are produced when electrons are disturbed in the respective orbital of an atom. This happens when a target element is bombarded with high energy electrons, accelerated charged particles or X-rays themselves. As a result, the electrons in the target element are knocked off the shells mostly the inner shell and electrons in the higher energy levels drop to fill the vacancy emitting excess energy in form of photons (characteristic x-rays) as they do so. This form of x-rays produced is known as continuum x-rays when an electron or

high energy charged particle loses energy upon passing through the coulomb's field of a nucleus and is called Bremsstrahlung.

Characteristic x-rays have discrete energies depending on electron energy levels with respect to shells, that is distinct energies; K, L, M, N, … however, K level energy is mostly considered in shielding purposes which is unique for every nuclide. X-ray sources in industries and medical field are machines with x-ray tube being common. They produce continuous bremsstrahlung x-rays up to maximum electron energy; that is, the voltage across the tube; with sufficiently high voltage being able to produce characteristic x-rays. The energy distribution depends on the voltage applied which will be equivalent to electron energy which can be up to 350 keV with modern technology, in terms of direction machines are directed toward the target unlike radionuclides which are isotropic. X-rays are categorized depending on peak voltage from 5-20 kVp are ultra-soft to very hard x-rays >250 kVp then there are those in MeV range produced by accelerators and betatrons (Data, 2011).

2.1.2 Gamma rays

Most radioactive processes are accompanied by gamma emission however, some other nuclides like ^{60} Co emit gamma naturally. In a fission reaction, gamma photons are categorized in to two groups, prompt gamma and delayed gamma, the former being photons emitted in the first Nano-seconds of fission reaction while the latter refers to those produced later by fission products. The prompt fission gamma spectrum is approximately constant at 6.6 photons MeV^{-1} $fission^{-1}$, where by the spectrum falls off sharply with an increase in energy.(Cacuci, 2010) Other common sources are artificial nuclides produced

mostly in nuclear reactors, when the nuclide is irradiated by neutrons, the nucleus can absorb the neutron and form a new nuclide.

The newly formed nucleus remains in excited state for some time depending on the nature of the nuclide and emit gamma rays which are known to be unique for each element thus this concept is used in neutron activation analysis for elemental composition. Just as the x-rays, the emitted gamma rays are the characteristic of the radionuclide. Gamma rays from decay are emitted with a unique energy spectrum for the element decaying(Reilly D,et al, 1991). Radionuclides have unique discrete energies, emitting radiation in all directions, and are kept in shielded containers. Gamma-emitting nuclides have energies in the range between 0.01 MeV to 17.6 MeV.

2.1.3 Source characterization

For different facilities, radiation sources used differ in sizes. In the medical field; sources used are relatively small in dimensions though they have high activities. They are kept in shielded containers. Dimensions for irradiation facilities such as food irradiation and sterilization of medical products have varying physical sizes but have extremely large activities(International Atomic Energy Agency, 2001).

The most important or more practical source is the point source, radionuclides emit radiation in all directions (isotropic) and have unique energies for instance, cobalt-60 with energies 1.173 and 1.332 MeV hence is not difficult to characterize them and the same goes for X-rays.(Shultis & Faw, 1979) A line is a series of points, when doing computations related to line source, a point source is first assumed and then integrated over the dimensions of the line source. In shielding, if the dimensions of the shielding wall are

3 times larger than the length of the line source then it is acceptable to treat a line source as a point source with the computation's percentage error being 0.9 %. The same goes for surface and volume source integrated over the surface and volume respectively. It is acceptable to assume all sources as point sources as long as they possess finite dimensions and the distance is large enough. For instance, a barrel full of radioactive waste, the further away from the barrel it can be assumed as a point source. Apart from the distance, the interaction of radiation with matter within the source volume should be negligible as the source strength will be reduced towards the target if the interaction is significant.(Cacuci, 2010)

If we consider all point sources in general, the source maybe characterized depending on its energy, direction (of which most sources are isotropic), and time. However, in shielding, time is not considered as an independent variable the reason being an extremely small time delayed between change in the source and the resulting alteration in the field which is negligible. Most practical sources are not monoenergetic but have an energy spectrum, when performing calculations this need a multigroup approach to characterize the source but also some modern methods including the Monte Carlo simulations are able to take care of that. In the present study collimated point source directed towards the shield is employed with discrete energy distribution.

2.1.4 Material characterization

There are several characteristics of a material to consider when utilizing the material as a shield. These include chemical and physical properties such as; particle size and shape, surface area and charge components, degree of substitution, the color, viscosity, plasticity, porosity, water absorption, radiation and thermal stabilities. According to (Chawla, 2013)

there are several techniques used to characterize materials; various microscopies electron and optical to mention a few, neutron activation analysis (NAA), Raman spectroscopy and others. In general, spectroscopy is the study of how radiation interacts with matter, it is applied as a tool to determine molecular lattice structures, chemical compositions and molecular lattice vibration frequencies. In most nuclear cases, NAA is employed which applies the concept of radiative capture to determine elemental composition. In shielding, the elemental composition and density of the material are important, and these are required in MCNP code to model the shielding material. The denser the material is the higher the photon shielding effectiveness hence concrete and lead are mostly applied as shielding materials, however other material can still be used if adequate thickness is employed, with lower costs and availability.

2.2 Attenuation properties of materials

Materials have unique properties which are useful in radiation shielding, this property is the density of the material, the higher the density the better the material is in attenuating radiation. One of the most important properties is the *linear attenuation coefficient* μ defined in equation (1), μ is the total of all possible interactions a photon can experience upon interaction with matter.

Main mechanisms in which a photon interacts with matter are the photoelectric effect, Compton scattering and pair production. In Compton scattering, a gamma ray interacts with an electron that is weakly bound, which does not need much energy to be set free thus a ray just loses its fraction of energy to the electron and remains free after collision

continuing in a deflected direction due to a collision. The electron also gains kinetic energy and it is set in motion. In pair production a gamma particle with energy exceeding 1.02 MeV happens to disappear going through an atom and passing near a nucleus, this particle re-emerges as two particles with a positive charge and negative charge referred to as positron and electron respectively. This pair is known as electron-positron pair.(Cember & Johnson, 2008) Both particles have approximately equal kinetic energies, and both have a mass of 0.51 MeV. These particles are mostly absorbed in matter due to reduced energy.

The photoelectric effect occurs when gamma particle loses all its energy in a single collision, the probability for this process depends on the energy of the incident gamma ray and the atomic number Z. The gamma particle can interact with a strong bound electron and disappears transferring all its energy, a fraction of the gamma energy is used to overcome the binding energy and the remaining fraction converted to kinetic energy which sets the electron free.(Nelson & Rewy, 1909)

$$\mu = \mu_{\text{photoelectric effect}} + \mu_{\text{Compton scattering}} + \mu_{\text{pair production}} \quad \ldots\ldots\ldots\ldots (2)$$

Mass attenuation coefficient (MAC) μ_m provides a measure of fractional attenuation per unit mass and it is independent of the density of the material, it is determined by dividing μ by the density of the material ϱ expressed in equation 3;

$$\mu_m = \frac{\mu}{\varrho} \quad \ldots\ldots\ldots\ldots (3)$$

The relationship between the linear attenuation coefficient and mass attenuation coefficient is expressed in equation (4). Interaction of photon with matter depends on the atomic

density of the material in question, the introduction of mass attenuation coefficient aids in making the computations independent of the density of the material. It is expressed in g/cm^2 or cm^2/g (H. Cember & Thomas E. Johnson, 2008)

$$\mu = \mu_m * \varrho \quad \ldots\ldots\ldots\ldots\ldots\ldots\ldots\ldots\ldots\ldots\ldots\ldots. (4)$$

transforming equation (1) to $I = I_0 e^{-\mu_m L}$ …………………………………. (5)

Within matter, interaction is statistical, the higher the density of the material, the higher the probability of interaction. Photons take various distances before interaction, the average distance a photon takes before the interaction is known as a *mean free path* λ.(H. Cember & Thomas E. Johnson, 2008.)

$$\lambda = \frac{1}{\mu} \ldots\ldots\ldots\ldots\ldots\ldots\ldots\ldots\ldots\ldots\ldots. (6)$$

The thickness of a material required to reduce the radiation intensity by 50 % of the original intensity is known as the half-value layer (HVL). It is appropriate to compute the number of HVLs of the shielding material required to reduce radiation levels to desired levels. Under good geometry where we do not consider buildup factors HVL is determined from equation (1) by;

$$\frac{I}{I_0} = \frac{1}{2} = e^{-\mu L}$$

$$ln\frac{1}{2} = -\mu L_{\frac{1}{2}}$$

$$L_{\frac{1}{2}} = \frac{ln2}{\mu} = \text{HVL} \quad \ldots\ldots\ldots\ldots\ldots\ldots\ldots\ldots \quad (7)$$

The number of HVLs (n) required to reduce radiation is given by;

$$\frac{I}{I_0} = \frac{1}{2^n} \quad \ldots\ldots\ldots\ldots\ldots\ldots\ldots\ldots\ldots\ldots\ldots\ldots \quad (8)$$

Tenth value layer (TVL) is the thickness of the shield require to reduce a radiation beam by to 10 % of its original value and can be determined by replacing half by one-tenth in equation (7). (Cember & Johnson, 2008)

2.3 CONVERSION INTO DOSE

Radiation has significant effects upon interaction with matter, either as directly or indirectly ionizing radiation such as x-rays, gamma rays and neutrons. Depending on the composition of the material, the effects vary from minor to worse. The knowledge of how energy is deposited within matter is important in radiation shielding as it aids in the evaluation of how much damage can occur such as void formation, irradiation creep, swelling and heating up of the material. Conversion of particle flux or energy flux to exposure rate and dose rate is needed to express exposure rate and dose rates to a standard unit, from MCNP tallies. The results are in terms of number flux descriptors: either surface flux particle flux per volume flux. American National Standards Institute (ANSI) made flux to dose rate conversion factors available in ANSI/ANS-6.6.1 1977 to be utilized by designers of new facilities for shielding purposes.

There are ways of converting energy deposited by photons in matter, these are indirectly ionizing radiation which deposit their energy in two stages.

1. The energy carried by photons is transformed into kinetic energy of charged particles such as electrons
2. Directly ionizing charged particles deposit their energy in the material by excitation and ionization

In MCNP, there are tallies used to determine how much energy is deposited in the material, that is tally F6 known as track length estimate of energy deposition.

Kerma (kinetic energy released per unit mass) is the amount of all kinetic energy transferred from uncharged particle; photon or neutron to primary ionizing particles per unit mass, it does not consider what happens afterwards, whether the energy escaped the material or is absorbed. But it aids in dose calculations since it tells how much energy is deposited per mass. The energy can be transferred in any of the mechanisms discussed earlier; Compton scatter, pair production, photoelectric effect or Rayleigh scattering. Mathematically defined as

$$kerma(k) = \frac{dE_{tr}}{dm} \ldots\ldots\ldots\ldots\ldots\ldots\ldots\ldots\ldots\ldots\ldots\ldots \text{(9)}$$

dE_{tr} is the sum of kinetic energies of all charged particles extricated by photons in a mass dm. Kerma can also be calculated from the mass-energy transfer coefficient of the material and the energy fluence. Mass-energy transfer coefficient is the MAC multiplied by the fraction of energy transferred from the interacting photons to charged particles. It is denoted by the following expression;

$(\frac{\mu_{tr}}{\varrho})$ where μ_{tr} is the energy transfer coefficient

The energy deposited per unit mass can be absorbed within the mass and some of the energy can leave the volume after interaction processes while some photons can pass through the shield without interaction. The quantity of energy absorbed within the material per unit mass is the *absorbed dose*

$$D = \frac{dE}{dm} \quad \ldots\ldots\ldots\ldots\ldots\ldots\ldots\ldots\ldots\ldots\ldots\ldots \quad (10)$$

The SI units Gray equivalent to Joule per kilogram, where dE is energy imparted. Before the introduction of SI units, the dose was measured by a unit called rad.(H. Cember & Thomas E. Johnson, 2008)

1 rad = 100 ergs/g

2.4 ADVANCES IN RADIATION SHIELDING METHODS

2.4.1 The transport equation

The photon transport equation effort is described by (Fano et al., 1951). Much of the effort dealt with the moment's method of solving the transport equation describing the spatial, energy, and angular distributions of particle fluences arising from fixed sources. The transport equation describes the photons through medium considering the change in photon distribution factor, that is, how many photons escape through boundaries, how many are absorbed within the medium, how many are scattered and how many are produced either straight from the source or produced in scattering processes. One of the modern methods involving computer codes is by using this equation to simulate the transport of the particles through a medium by Monte Carlo methods.(Cacuci, 2010)

If we consider a small unit volume dv within a medium, with the direction of radiation beam being s;

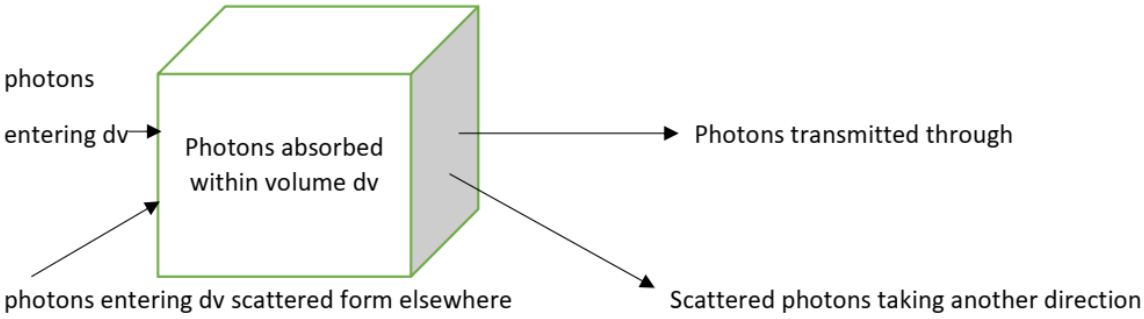

Figure 2.2 Schematic diagram of possible movements of photons within an infinite volume. (S. Andersson, 2012)

$$\int_v^\infty \frac{\partial N(r,s,t)}{\partial t} dv = -\int_v^\infty cs.\nabla N(r,s,t)dv - \int_v^\infty c\mu_s(r)N(r,s,t)dv -$$

$$\int_v^\infty c\mu_a(r)N(r,s,t)dv + \int_v^\infty c\mu_s(r)\int_{4\pi}^\infty p(s'.s)N(r,s',t)d\omega' dv + \int_v^\infty q(r,s,t)dv$$

…….. (11)

The term on the left-hand side of equation (11) represents the distribution of photons with respect to time t, whereby the number of photons N depends on direction s, time t and position r. The terms on the right-hand side are either negative or positive, negative terms

are loss modes or photons removed from the main beam, the first term on the right represents photons through the boundary surface c expressed in Gauss' theorem. The second term represents photons lost through scattering and the third term represents photons lost by absorption where μ_s and μ_a are coefficients for scattering and absorption respectively.

The positive terms are source modes, the first term for positive terms takes care of photons gained through scattering joining the main beam, $p(s'.s)$ is the probability function for scattering from main direction s to any direction say, s' and the last term is the source term. The movement of the particle in a medium is statistical with several possibilities, the transport equation aid in predicting the fate of the particle within the medium, since nothing is exact; there is mean free path which is an average distance travelled by a particle between successive interactions and there are different forms of interaction which are all probabilities depending on defined parameters such as cross sections and attenuation coefficients.

2.4.2 Buildup factors

If we consider any point within a medium or a shield where photons are propagating, the number of photons that reach that point have experienced different interactions to get there. Since the transport of photons is statistical, some photons get to the point without any interactions and there is also a group which has experienced numerous scatters ranging from one to any number greater. The buildup factor B(r) as shown in equation (12) accounts for scattered photons which after being scattered still progress through the shield these factors are significant in poor geometry (broad beam). Buildup factors depend on the

number of mean free paths within the medium to the point of interest and depend also on source geometry; whether monodirectional or isotropic, plaque source, volume source or point source. The buildup factors have values which are greater than one up to large values, the values depend on the material and the source geometry.

Data for buildup factors has been made available in the literature for futures designs of radiation facilities (Lištjak, Ondrej, Kubovi, & Vermeersch, n.d.). Generally, the buildup factor accounts for secondary gamma radiation and thus equation (1) can be modified by the introduction of buildup factor B;

$$I = I_0 B e^{-\mu_l L} \quad \text{..... (12)}$$

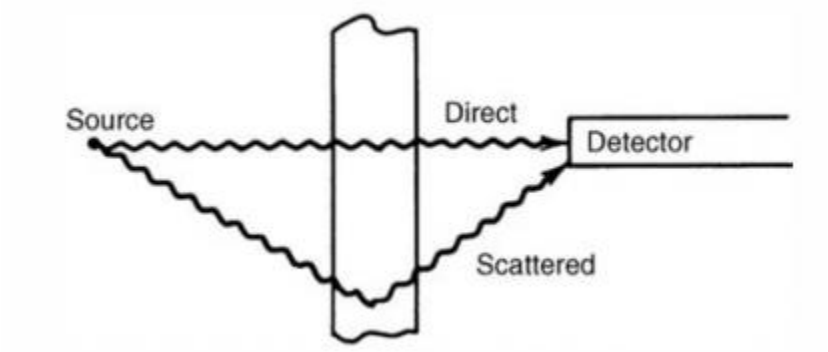

Figure 2.3 shows that the scattered radiation contributes to the transmitted radiation. (Glenn F. Knoll, 2010)

.

Various buildup factors were formulated from the analytical method to computerized methods. These represent ratios of the total dose, scattered dose plus uncollided dose, to

that of uncollided particles only. Refinements in the computation of buildup factors continued to be made over the years. An adjoint moments method code had come into use (Simmons 1973) and treatment of positron annihilation had been incorporated (Morris et al. 1975). Working with buildup factors computed using the PALLAS code, Harima developed a data fit in the following form, called the *geometric progression* formula (Harima 1983; Harima et al. 1986, 1991).

Two more foundation stones need to be in place to support a mature radiation shielding technology. One is a comprehensive set of cross sections, or interaction coefficients, accounting for not only reactions but also dosimetry related coefficients such as those for energy deposition. Another is a set of fluence-to-dose conversion factors applicable to a comprehensive array of dosimetry conditions.

2.4.3 Material cross section

Cross section σ of a material is the probability of certain interaction to occur, it depends on the chemical composition of the material, some elements have high absorption cross-section for photons while some have high scattering cross section. This parameter is very important in shielding, for instance, to shield fast neutrons, first, they are slowed down by materials with high scattering cross sections, then absorbed by a material with high absorption cross section for neutrons and then heavy material absorb associated gamma.

There are data libraries made available in literature resulting from various evaluations since the utilization of radiation. (Shultis & Faw, 1979) Cross section data is available in ENDF/B-6 (evaluated nuclear data file), this contains computed cross section for different

elements, spectra, angular distributions, products of fission reactions, photo-atomic and thermal scattering law data. (Shultis & Faw, 1979) This ENDF/B-6 has been maintained by the cross-section evaluation working group (CSEWG). This data is used in modern designs and analysis computer codes such as MCNP (X-5 2003). The other institute is the National Institute of science and technology (NIST) which has been responsible for gamma-ray interaction coefficients.

Storm and Israel 1967 and Pelchat et al. 1981 provided another set of cross sections for photons which have been mostly utilized since their introduction because they take energy transfer and absorption cross section into consideration and thus help evaluate fluence to dose conversion factors. For gamma-rays, fluence to dose conversion factors for localized values of exposure can be calculated from readily available data of energy deposition coefficients for air, tissues and other media.

The results from monte Carol methods and other methods are in terms of particle fluences, energy fluences and radiation fields and these do not indicate the quantity of danger defined by doses, quantification is important for estimating the risks such as heating up of the material or stochastic health effects or deterministic effects. Specifically, Monte Carlo methods yield the energy spectrum and thus it is necessary to convert into dose by utilization of fluence to dose conversion factors. These coefficients are categorized into two groups one of its components were discussed earlier; kerma, exposure and absorbed dose under the group termed local conversion coefficients.

The other class is referred to as phantom related coefficients, these are coefficients which aid in risk evaluation in terms of average doses or effective doses making use of point fluences and dose with anthropomorphic phantoms. Phantoms are used to model real

materials including human tissues to calculate doses such as operational dose; ambient doses, effective doses and personal doses. There are anthropomorphic phantoms and geometric phantoms and their difference is that for geometric phantoms the calculations of doses are done at a point of fixed depth while for anthropomorphic the dose is calculated as an average over specific tissues and organs. Dose conversion factors are available in 1987 and 1996 reports of NCRP, in MCNP code either kerma or absorbed dose can directly be calculated by the different special tally specification or can otherwise be computed from energy-dependent fluence by use of dose conversion factors.

2.4.4 Monte Carlo Methods

The Monte Carlo method of simulating radiation transport computationally has its roots in the work of John von Neumann and Stanislaw Ulam at Los Alamos in the 1940s (Taylor, 2012). The processes of scattering and absorption of photon transport are given by transport equation and Monte Carlo methods describe the fate of each individual photon. Monte Carlo methods can model complex problems which cannot be solved by deterministic methods even though they are sometimes considered to be time-consuming as the computer simulations can take a while before giving a solution. From equation (16), the transport equation involves many integrals which are integrated numerically, however, this procedure is hectic as each order of scatter produces four additional variables of integration, three spatial and one energy. Monte Carlo method is employed to simplify this procedure, the method reduces each integral to a single point numerical quadrature in which the point is picked randomly. For complex models, it is enough to randomly apply

the sampling process to the three spatial variables. The whole source is characterized by its effect at a single point. (Taylor, 2012)

Source strength is reduced to an equivalent point source in terms of most probable values of fluxes at each order of scattering. Monte Carlo methods use a probability density function (PDF) which accurately model the interactions within matter if the source involves energy distribution the multigroup method is utilized at constant cross section giving average probabilities for a particle in a specific group producing a secondary particle in another group.

Monte Carlo methods can take hours up to days to complete one simulation, high-speed computers have been introduced over the years since the introduction of computers this helped reduce time taken, however, there are complex simulations representing some rare events which can take an infinitely long time to execute one run even with modern computers. *Variance reduction techniques* have been introduced to reduce the long time so practical times and improve efficiency Monte Carlo methods.

There are techniques such as antithetic sampling and stratification, for stratification sampling, the domain D (which is the material) is divided into regions and sample of points are taken on each region and the results are combined to get the solution, this is better than considering the whole material with infinite points because each subregion gets its fair share of points to get a good answer and this simplifies the domain for integrals. (Kleijnen et al, 2010.)

In Monte Carlo methods, the averages of integrals are used which result in cancellation of errors by the randomness in the algorithm and antithetic technique tries to get even more

cancellation, these sampling techniques give the best answer from just a single pair of function evaluations. Figure 2.4 below demonstrates the basic journey of photons through matter, photons come from the source and are transported through the matter, they interact with matter with the mechanisms discussed earlier in this chapter. In the scattering process some secondary particles are born and join the transported photons and in turn also undergo interaction processes while some particles escape the medium in various directions

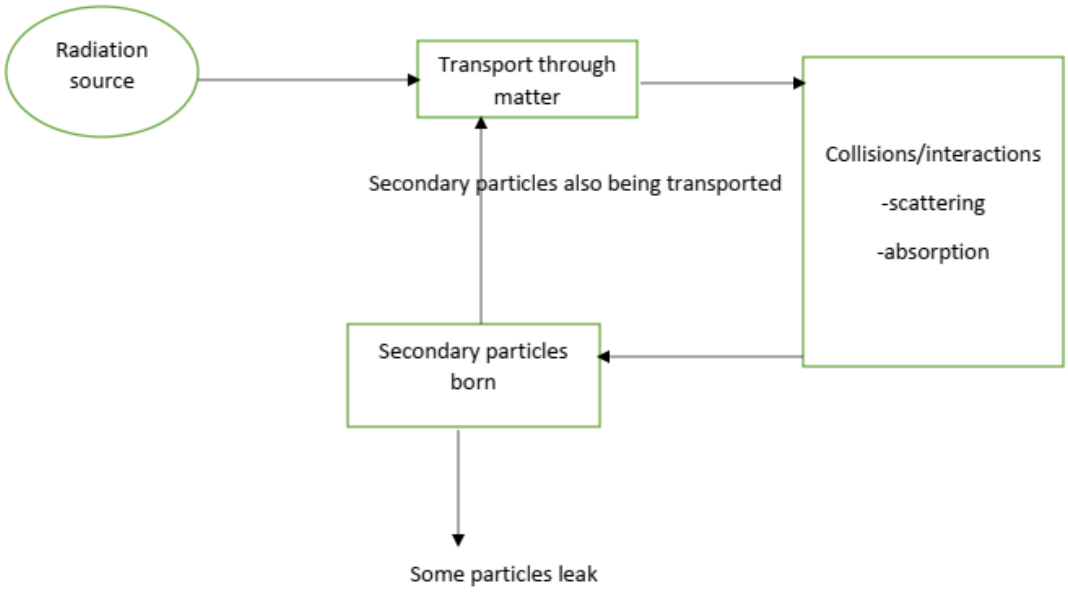

Figure 2.4*:* a simplified random movement for an individual particle in a Monte Carlo method. (Brown & Martin, 1984)

Advances in Monte Carlo calculations were also made. The MCN code was merged with the MCG code in 1973 to form the MCNG code for treating coupled neutron-photon transport. Another merger took place with the MCP code in 1977, allowing detailed

treatment of photon transport at energies as low as 1 keV. This new code was known, then and now, as MCNP. MCNP has gone through a series of improvements adding new capabilities and improvements, such as new variance reduction methods, tallies, and physics models. New releases appear every few years, and the version as of this writing is MCNP-6. It has also spun off a second version MCNPX with a capability of treating 34 types of particles with energies up to 150 MeV.

2.5 RADIATION SHIELDING TODAY

Advanced methods and designs are introduced at a high rate since the 1940s, based on cutting costs, using available non-toxic and effective materials. Detectors are used to quantify radiation and responsible organizations give permissible doses, and ways to keep radiation as low as reasonably achievable (ALARA), quantifying leakage radiation, scattered radiation and primary radiation. More powerful radiation sources are now being employed with x-rays going as high as 350 keV. Availability of quantifying instruments led to simpler ways of designing shielding with qualified experts in the area of radiation protection making data for thicknesses of different shielding materials available; materials such as lead, concrete gypsum and more. The investigations on different materials are either done with deterministic methods or Monte Carlo methods before making recommendations to radiation facilities.

Modern radiation shielding analysis requires full-scale treatment of scattered particles as is done in the Monte Carlo and discrete ordinates computer codes. As computational resources grow, these more advanced transport methods become available on the desks of

office, classroom, and home. There are new developments of graphical user interfaces to assist users of codes such as the MCNP code.

2.6 CHALLENGES WITH AVAILABLE SHIELDING MATERIALS

Almost every country in the world has at least one radiation facility and planning to build more but not every country has materials that are being employed as radiation shielding materials today. Many countries have different materials possibly able to shield radiation but with unavailable data for shielding purposes. Factors leading to utilization of the material include low costs, availability, and the shielding properties of which theoretically all materials can be employed as radiation shielding materials.

Unavailability of concrete, lead, tungsten, gypsum and few other shielding materials is a major challenge in many countries. Lead is not easily machined due to its malleability and it is toxic, though concrete is available in most places, it is most effective in neutron shielding relative to gamma and x-rays which are of concern in the present study and it also needs boron to enhance its shielding effectiveness for neutrons. Materials incorporated with lead are very heavy and this is a challenge when referring protection materials such as garments, curtains and cloves and there is a need to couple lead with cheaper materials.(Davraz, Pehlivanoğlu, Kilinçarslan, & Akkurt, 2017)

2.7 SHIELDING MATERIALS OPTIMIZATION METHODS

Shielding materials are selected based on low cost, nontoxicity and photoelectric absorption coefficients, lead being most efficient material due to its high density, it is not produced in every country in the world, thus there is a need to employ non-lead materials.

Optimization methods for non-lead materials are to increase their shielding effectiveness and minimize other bad properties such as toxicity and unstable irradiation properties. Most non-lead materials are utilized as bilayers or multilayers, the multilayer optimization method is common in neutron shielding since there is a need to slow down neutrons, absorb them and absorb the associated gamma emission.

However, for gamma rays and x-rays bilayers and multilayers are employed to increase the effectiveness of the shield with different materials and the composition of different materials can decrease the weight of the shield. Multilayer shields are utilized for narrowing X-ray energy spectra for instance, when a 3-layer shield has been used for ages composed of tin, copper and aluminum having tin first then copper and finally aluminum. Each next layer absorbs the characteristic x-rays of the preceding layer. In optimizing the shielding material there should be a balance in radiological protection, costs and sociopolitical factors. Cost-benefit analysis method in one of the optimization methods in terms of economical purposes, the aim is to provide maximum radiological protection at a minimum quantity of materials at low or minimum operational costs. Shielding optimization is also done by designing maze shields so that x- and gamma rays undergo multiple scatterings and attenuations while going through a maze. MCNP code is employed to optimize the thickness of the materials either multilayers or a single layer of each material by dividing materials into sub-sections and increasing the thickness gradually while examining the flux.(Chen & Wang, 2011)

2.8 COST-BENEFIT ANALYSIS (CBA)

The cost of shielding is one of the major factors to consider when constructing a nuclear and radiation facility. When choosing radiation shielding material, apart from attenuation properties, chemical and physical properties, irradiation and corrosive stabilities, there is a need to evaluate the costs and benefits of employing that material. Cost-benefit analysis is an important tool to evaluate the costs and benefits and the objective is to find a positive net benefit (equation 13); (ICRP 37, 1983)

$$B_s = V - (P + X + Y) \quad \text{.....(13)}$$

Where B_s is the net benefit of employing the material, V represents gross benefit, P stands for production costs where the protection costs are excluded, X accounts for costs for achieving the accepted level of protection and finally Y accounts for costs detriment (risk) of the utilization of the material though it's a challenge to quantify the damage thus debatable.

If B_s is negative the practice is ruled out; CBA aid in ensuring that the benefits are more than total detriment associated with the practice, in the present study, also compare with materials that are being used today. Radiation shielding is one of the parameters considered in radiation protection alongside with parameters such as exposure rate or occupation time for workers and others, the major objective why optimization is done is to determine optimum values for the mentioned parameters. The optimum protection (shielding) is determined by maximizing the net benefit (equation 13) with respect to a relevant variable such as collective Dose S, such that $(dB_s/dS) = 0$.

If it is assumed the P and V are constants in equation (13) then the optimization condition is achievable S_0 and this would mean that the cost of protection per unit dose balances the reduction of damage per unit collective dose (ICRP, 1983). To optimize radiation protection, one can be limited to the best combination of X and Y by minimizing their sum as a function of w where w is the parameter of radiation protection such as shielding thickness.

There are more parameters that must be considered as only shielding and occupancy time were mentioned earlier, parameters such as the number of exposed individuals and lifetime of installations of shielding. The other assumption made relating these parameters is that, there is an exponential relationship between dose rate and thickness of the shield. If ρ is the constant ration between the average dose rate and maximum dose rate, then the dose rates will be exponential with respect to the thickness of the shield, thus the cost of detriment Y for equation (13) can be assumed to be related to the thickness of the shield exponentially as shown in equation (14):

$$Y(w) = \propto N f_t \tau \rho H_u e^{-rw} \qquad (14)$$

α is the dimensional constant expressing the cost assigned to the unit collective dose,

N is the assumed number of exposed personnel.

f_t is the time spent at the exposed area.

τ is the lifetime of the installation , H_u is the maximum effective dose-equivalent rate experienced at an external face of the initial minimum thickness of the shield and r is the attenuation coefficient leading to the reduction factor being defined as e^{-rw} (ICRP, 1983) where w is the thickness of the material.

The cost of the installed or to be installed shielding materials are included alongside the support installation to make the total cost of the shield. It is assumed that from minimum thickness to optimum thickness of the shield, the thickness of the shield X_s is proportional to the quantity of shielding material as shown in equation (15) below:

$$X_s = X_v V_s + X_I \quad \text{..... (15)}$$

X_v accounts for cost per unit volume of the material, V_s denotes the volume of the material and X_I accounts for support installation costs and it is assumed to be constant. The cost of the shield can be expressed in linear form as shown in equation (16) since the volume and the thickness of the shield are coherently proportional to each other. If the rectangular planar is considered as the geometry for shielding the cost can be expressed as follows:

$$X(w) = X_v hlw + X_I \quad \text{..... (16)}$$

Where h is the height of the shield and l is the length while w is the thickness or the breadth of the planar.

Optimized dose reduction factor can be derived from equations (14) and (16) by minimizing the sum Y(w) + X(w) so that:

$$e^{-rw} = \frac{X_v hl}{\alpha N f_t \tau \rho H_u r} \quad \text{..... (17)}$$

CHAPTER THREE

MATERIALS AND METHODS

This chapter describes the materials and methods used to conduct the research work.

3.1 MATERIALS

Materials and software probed in this study are as follows:

- Southern pine wood
- Sandstones
- Clay
- Lead
- Monte Carlo n-particle transport (MCNP) code

3.1.1 WOOD

Wood is the most utilized material in the entire world, about 43 % of the world's consumption is in Asia, while Africa consumes 31 % and America 4 % (Koddenberg, 2016). Southern wood pine has been mostly used for construction, furniture, cabinetmaking and other things such as for decorative veneers. Soft wood such as southern wood pine is good for furniture making, its bending and stiffness properties are low, southern wood pine has a low resistance to shock and crushing strength. It is known for taking nails very well and can be glued without complications. There are old buildings and other constructions

made with southern pine wood in Lesotho which are still standing till today. Like any kind of wood; it is treated to prolong its construction life and enhance applicable properties.

Southern pine wood is composed of carbon, hydrogen and oxygen which is common for most types of woods. Materials containing hydrogen and carbon are known for their effectiveness in shielding and mostly preferred for neutrons though still used for photons because they can lower the energy of a neutron upon successive collisions. In studies done before, it was found out that wood properties are comparable to those of gypsum and brick which are already being employed in radiation shielding. (Aggrey-Smith et al, 2016) southern pine wood and most types of wood have significantly low induced radioactivity upon irradiation hence less hazardous to human life and exposure of wood to very intense gamma radiation can lead to decay, mechanical properties of wood vary according to temperature, increasing when cooled otherwise decreasing. Chemical composition of wood differs for each part, that is, for the stem, roots, and branches and from type to type. Generally, wood is composed of about 50 % carbon, 6 % hydrogen, 44 % Oxygen and traces of some metal ions and the same goes for southern one wood.(Pettersen, 1984)

The density (g/cm^3) of wood (southern pine, common in Lesotho southern Africa) = 0.64000, total atom density (atoms/b-cm) = 4.932E-02. Detailed elemental composition and MCNP form are shown in appendix A.

3.1.2 CLAY

Clay minerals have been involved in current research studies, in nuclear, clay has played an important role in radiation protection as it has been used to accommodate high-level

waste (Morari, 2016). Clay is one of the abundant minerals in the world and thus has become the main component of repository facilities. The rocks and clay are the oldest building materials, clay can be made into ceramic form enhancing its mechanical properties, when wet clay has plastic quality allowing it to be fabricated into various shapes. Clay is dried and becomes very hard as a rock; the hardening is mostly achieved through heating thus resulting in a ceramic form

Ceramics have various applications such as floor tiles, bricks for building and pots to mention few, due to its strength, availability, ability to be used as a building material and low induced radioactivity under radiation, clay can be used as a radiation shielding material if its properties are known. Clay has the density (g/cm^3) = 2.2000 and total atom density (atoms/b-cm) = 6.333E-02, accurate at about three significant figures.(McConn, Gesh et al, 2011) A complete table showing atomic density and MCNP form of integrating clay in the code are in Appendix A.

Chemical composition of clay includes oxygen, sodium, magnesium, aluminium, silicon, phosphorus, potassium, calcium, manganese and iron and oxygen, aluminium and silicon contribute larger fractions followed by iron. Clay in Lesotho has been used for decades on the walls of traditional huts, for strong pots which lasts for years in ceramic form. In Lesotho, kids play with clay making playing cows and cars these things are very hard especially if one can burn them, this strength of clay really calls for investigation on radiation shielding effectiveness and its ability to be used for depository of radioactive materials propose for utilization in radiation shielding.

3.1.3 SANDSTONES

The other fascinating rock that has been employed for ages in construction is the sandstone, this is one of the most utilized sedimentary rock in Lesotho with its quarry situated at the place called Lekokoaneng Berea Lesotho where the bricks of various sizes are made and distributed over the country. It is mostly used for building and fencing; the quarry has been of importance even to the economy of the country as it even crosses the border to South Africa. Sedimentary rocks are classified depending on elemental composition and particle composition that is;

I. Siliciclastic sedimentary rocks; sandstones, conglomerates, shales
II. Carbonate rocks; limestones and dolomitic

The composition of sand and that of sandstone is similar, typically consisting of quartz which is a major porosity-destroying cement in sandstones (Morad, 2000). Sandstones withstand very harsh conditions such as extreme temperatures, acidic conditions and alkaline conditions. These rocks are composed of fragments of minerals held together by a mineral cement; they absorb water at the capacity of not more than 1 % with negligible porosity which can make it a quite good material for radiation shielding. Sandstones are known of their strength in construction, there are some very old walls in India built with sandstone and are still firm and this rock is known for making very strong floors.

The density of sandstones is estimated to 2.320000g/cm^3 and the total atom density is about 7.166E-02atoms/b-cm with the elemental composition including lead, iron, tin, calcium, potassium, sulfur, silicon, aluminium, magnesium, sodium, oxygen, carbon and hydrogen. The sandstone in Lesotho is white in colour, it has almost negligible porosity which makes it almost impermeable, advances in shielding led to also consider the floor

when designing facilities, sandstones are known for very strong floors in Lesotho just as the strong walls which have been standing for years; old school buildings, churches built by missionaries and old university buildings. It has excellent compressibility strength, with low absorption of water as well as being fireproof which makes it more common in construction than wood and its floors are non-slippery.

3.1.4 Lead

Lead has been a very essential material for both gamma and x-ray shielding since the beginning of the application of radiation technology. It has been used as the containment for radiation sources as well as making shielded walls and glasses for protection of operators, patients and public. The main property that makes lead an ideal material for shielding is its density, it is very dense having a density of 11.35g/cm^3. However other properties that contribute to the effectiveness of the material of which lead possesses most are; properties such as degree of flexibility, stability under intense radiation and extreme conditions, high atomic number.

Lead can also be made in many forms brick, wool, glass, pipes and many more, lead is highly effective and mostly used as the reference material to weigh the effectiveness of other materials to be used in radiation shielding, and that is the reason it is used in this work.

3.1.5 MONTE CARLO N-PARTICLE (MCNP) TRANSPORT CODE

MCNP transport code is a very powerful computational tool used to simulate particle transport. Unlike the deterministic methods which do not involve randomness but rather solving a specific equation such as transport equation, Monte Carlo method simulates

individual probabilistic events involving a particle. This code is useful in providing a solution to complex problems which cannot be solved with computer codes not involving randomness.

MCNP code is used in radiation protection and dosimetry, radiation shielding, radiography, medical physics, nuclear criticality safety and so on. The neutron energy is from 10^{-11} to 20 MeV while it is from 1 keV to 100 GeV for photons. MCNP is used to compute neutron population from generation to generation in research reactors and power reactors, it is also used to compute x-rays and gamma doses in radiation protection and dosimetry. The user creates an input file describing the source, the target geometry, the detectors or the types of tallies desired, K code for reactors and the surrounding(Kafi et al, 2005).

3.2 METHODS

The MCNPX version 2.6.0 code was used as a tool to trace the fate of nuclear particles as they pass through some selected materials to determine transmission factors and thicknesses of materials required to reduce radiation to acceptable doses. The slab geometry was employed throughout the computations and this was employed first for wood with its elemental composition shown in Appendix A with reference to [R. J. McCann, 2011].

3.2.1 SLAB GEOMETRY FOR POINT, CYLINDRICAL AND PLAQUE SOURCE

The simulation was done on wood, clay and sandstone selected based on their potential as shielding materials and their availability in Lesotho. The first source was the cobalt 60 (gamma source) point source considering a bad geometry for practical purposes.

Three MCNP codes were written, all the same in terms of modelling only differing by materials considered; that is, there was a code for wood, for clay and for sandstones. The modeling for each material and the procedures are summarized below. Before any material could be used the dose was recorded at the same distance without the shield.

The 10 cm thickness material slab was 50 cm away from the source and two-point (ring) detectors defined by tally 5 (f5: p) in MCNP, both were at 30 cm distance beyond the shield and 5 cm apart. The model was in such way that the source was placed in the rectangular 'room' along the x-axis, the shielding slab (wall) was at the origin and the source was directed to it. There was a small adjacent room where the locations of two detectors were, the model is shown in Figure 3.2. Coherently, between the source and shielding material and between the shield and the detector there was a second material being air and therefore this was considered in the cell card where the density of air was taken to be 1.225E-03 g/cm^3. The simulation was done in photon mode for each material beginning with 10 cm thickness, the flux tally for the 2 points were taken and added to take an average.

The source geometry was altered to a cylinder, the cylinder had the radius of 1cm and height of 50 cm extending from the floor to the roof of the source cell as shown in Figure 3.2, the shield was 50 cm from the centre of the cylinder, with the detectors placed 30 cm beyond the shield as in point source. The cylindrical source was along the z-axis, the

simulations were done for each material with 10 cm initial thickness for each and 5 cm increment, the source was then changed to a rectangular plaque with other parameters such distance from the source to the shield and form the shield the detectors unaltered. The plaque source perpendicular to the x-axis, the height and length both extending from 0 to 50 cm same as dimensions of the source cell. The same procedure followed for point and the cylindrical source for all materials.

The computations were done in photon mode only in MCNPX which uses ENDF/B-VII.1 nuclear and atomic data, the ring detector was placed at points 30, 30, 30 and 30, 25, 25, after each simulation, the records were taken, and the material thickness incremented by 5 cm for the next simulation. As the material became thicker, it was divided in smaller slabs of 5 cm each and setting cell importance for each sub-slab to apply variance reduction modelling methods to improve the computation efficiency.

3.2.2 X-ray Source

Still using a slab geometry, the source was now replaced by the X-ray source with strength up to 300 keV divided into two ranges for different applications, being 60-120 keV for medical applications and 120-300 keV for other industrial applications, however taking minimum and maximum energies in each range, point source was the only source geometry applied for x-rays. The same geometry and distance were utilized but changing the initial thickness of each material. The changing of the initial thickness of the materials is due to lower energy of x-rays as compared to gamma rays from cobalt 60, the initial thickness of wood was 5 cm incrementing with 5 cm each step up to 50 cm.

Clay and Sandstone have high density as compared to wood hence the initial thickness of clay and sandstone was lowered to as low as 1cm in order to obtain the HVLs of the two materials, the initial thickness was 1 cm then 2 cm was used next with 5 cm being used after 2 cm, from 5 cm to 40 cm the increment was 5 cm as before. The same material atomic composition with reference to Appendix A. The X-ray source was still a point source taking the minimum and maximum energy for each range. Figures 3.1 and 3.2 shows the source-detector geometries and 3d model in MCNP visual editor.

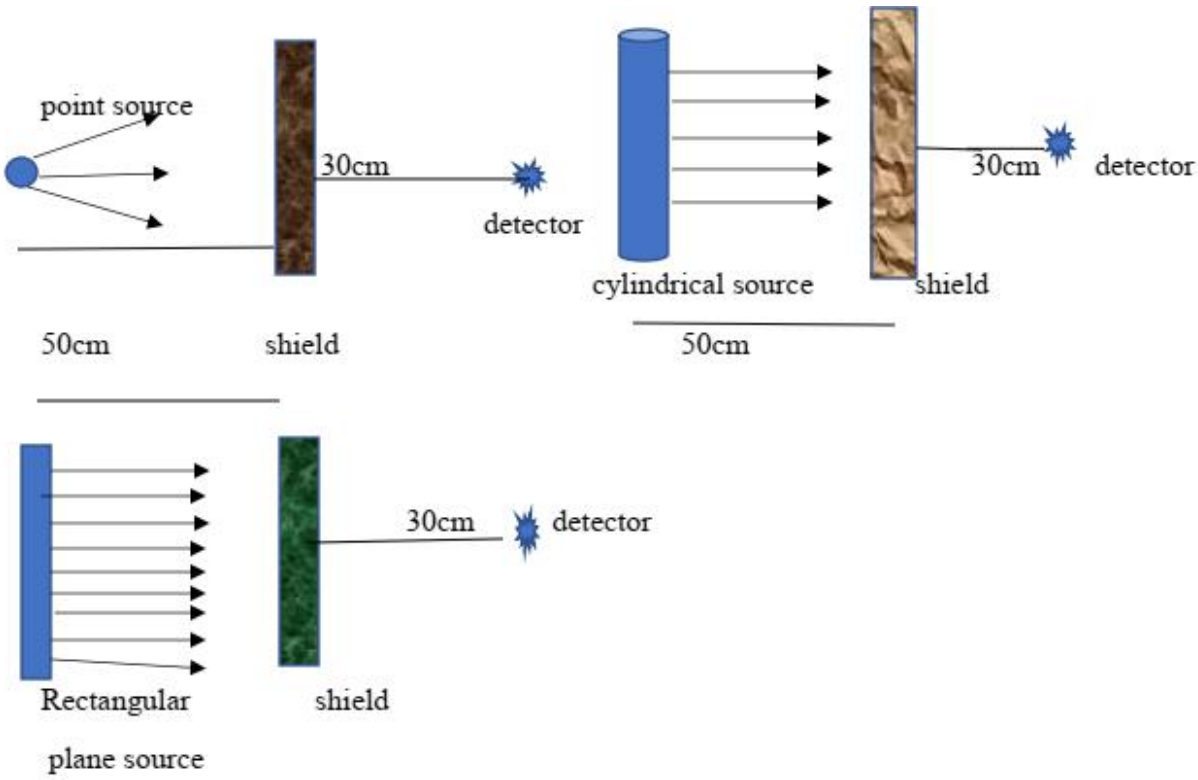

Figure 3.5: top left; consists of the point source, detector & the shielding material, top right; the source is a cylindrical source, bottom left; the source applied is the rectangular plane source.

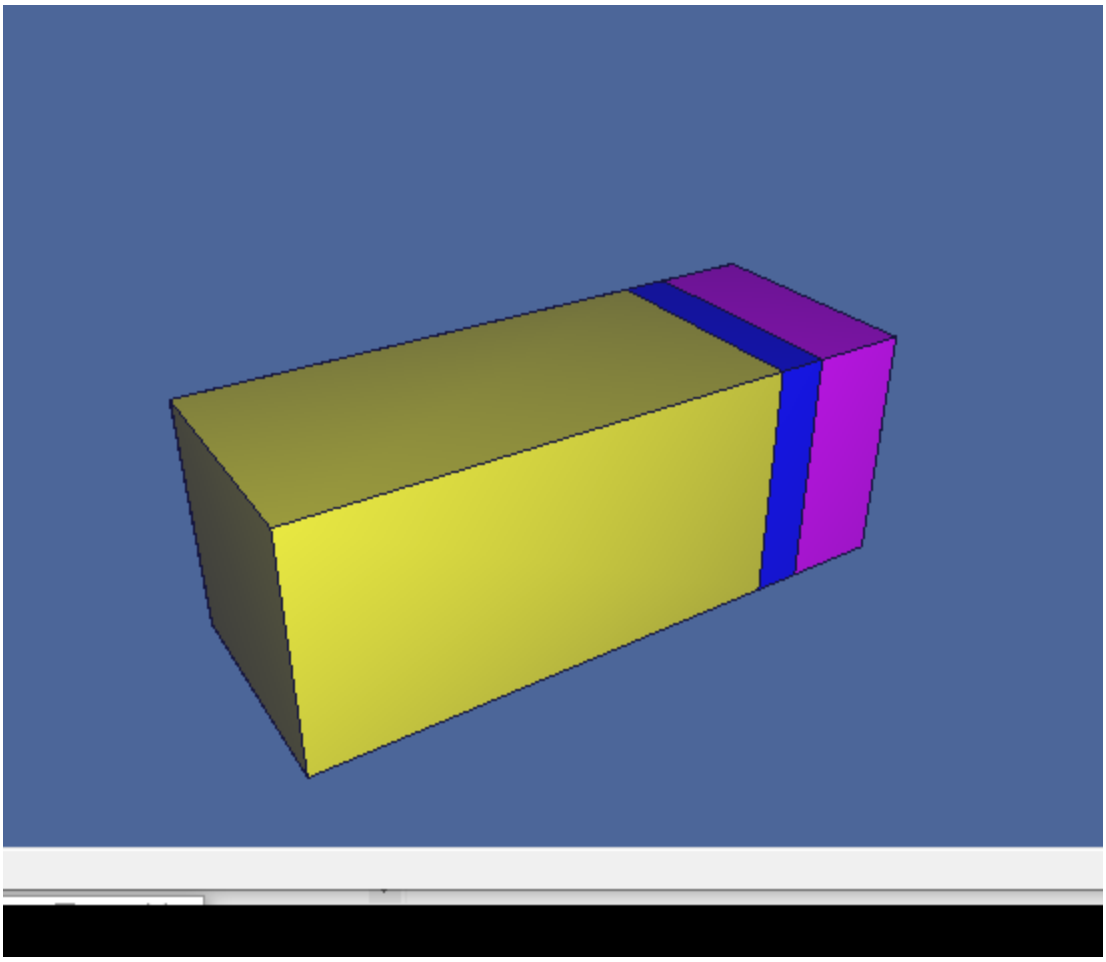

Figure 3.6 3D model of the MCNP input, the yellow cell is where the source is located, the blue cell is the shield and the blue cell is the cell beyond the shield, that is, the detector region.

3.3 Calculations

To determine the shielding effectiveness of the material, mostly a graph is used where the thickness is plotted against the transmission. If we define the $F_{E,D}$ as the flux recorded behind a particular shielding material of thickness d for a source with energy E, the the corresponding transmission factor $T_{E,D}$ can be calculated using the following equation;

$$T_{E,D} = {}^{F_{E,D}}\Big/_{F_{E,0}} \quad \text{..... (18)}$$

Where $F_{E,0}$ is the initial flux (with no shield).

To determine linear attenuation coefficient equation 1 was used;

$$I = I_0 e^{-\mu L} \quad \text{..... (19)}$$

Rearranging the equation to obtain a linear attenuation coefficient leads to;

$$\mu = \frac{1}{L} ln \frac{I_0}{I} \quad \text{..... (20)}$$

Mass attenuation coefficients were computed by dividing the linear attenuation coefficients by material densities.

Buildup factors (B) were also computed by using the following equation:

$$B = \frac{total\ photon\ flux}{uncollided\ flux} \quad \text{..... (21)}$$

CHAPTER FOUR

RESULTS AND DISCUSSIONS

In this chapter, the results obtained from this research work are presented and discussed.

4.1 Cobalt- 60 point source

Figure 4.1 shows the attenuation curve of wood, clay and sandstone for gamma rays from cobalt- 60, without the shield, the flux detected was 1.07E-05 photons /cm^2. Starting from the initial thickness of 10 cm through to 50 cm thickness, 6.94E-01 (69.4%) of the initial radiation was transmitted through 10 cm thick wood down to 1.43E-01 (14.3%) for 50 cm thick wood shield. Lead has been used as the reference material for other materials over the years since the initiation of radiation shielding, according to Figure 4.2 which agrees with the results obtained by (F.S Kirn 1954), 14% transmission of cobalt 60 gamma rays is achieved through at least 3.7 cm thick lead shield and that would mean 50cm wood shield would correspond to 3.7 cm thick lead shield.

Figure 4.1 Transmission of cobalt 60 point source through wood, clay and sandstone.

To transmit 50 % of the gamma rays from the cobalt 60 source, according to the curve in figure 4.1, one would require 18 cm thick wood (which can be referred to as half value layer) which can provide the same protection as 1.2-1.5 cm thick lead shield (HVL) as the results shown in figure 4.2. Since in radiation protection is even better to overshield 20 cm can be preferred over 18 cm. according to the curve in figure 4.1 the tenth value layer seems to be beyond 50 cm thickness, however, using the logarithmic interpolation as shown in figure 4.1, it was found that the TVL of wood is 56 cm thickness correspond to 4.2 cm thick lead. The lower density of wood is the reason for larger thicknesses being needed to attenuate gamma rays, however, the fraction transmitted gradually decreases as the thickness of wood was increased.

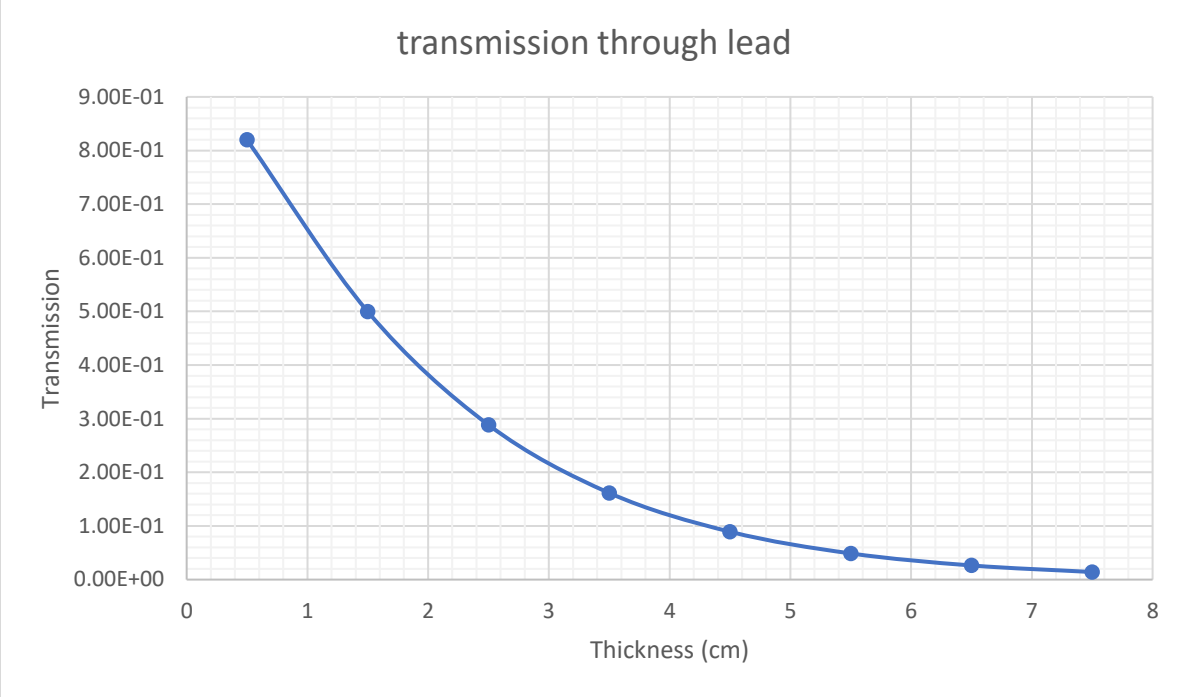

Figure 4.2:Transmission of cobalt 60 point source through the lead slab.

The transmission through clay shield is also demonstrated in figure 4.1, the value of photon flux in the absence of the shield was still 1.07E-05 photons/ cm^2. The minimum or initial thickness of clay was 10 cm which transmitted the fraction of 4.83E-01 (48.3 %) of the cobalt 60 gamma rays. The value is relatively low and better as compared to wood at 10 cm thickness which makes sense due to the higher density of clay. The maximum thickness which was 50 cm transmitted 6.51E-03 (0.65 %) of the gamma rays.

Clay is more effective relative to wood coherently due to its heavy mineral content and higher density. Comparing it to lead which is used as the reference material, 9.5-10.5 cm thick lead is require to transmit 0.6 % of cobalt 60 gamma rays as shown in figure 4.2 which corresponds to 50 cm thickness of clay. Determining the HVL and TVL of clay, according to figure 4.1, although the curve of the initial thickness of clay began with 10

cm it can be determined that 9 cm thick clay shield is required to transmit 50 % of cobalt 60 gamma rays as 10 cm thickness of clay transmitted 48.3 %. This HVL corresponds to 1.5 cm thick lead shield according to (Kirn 1954).

Ten percent of the gamma rays can be transmitted through the 25 cm thickness of clay which was the TVL as compared to 4.2 cm thick lead. The thicknesses of clay required to give the same result as wood is very low, HVL of wood, for instance, was 18 cm while for clay was 9 cm , TVL of wood was 56 cm while for clay it was 25 cm.

The transmission through sandstone shield was somewhat comparable to that through clay shield, coherently due to their slightly different densities with clay having 2.2 g/cm^3 and sandstones having 2.32 g/cm^3. As shown in table 4.1.3 and Figure 4.1, the thickness of sandstone started from 10 cm in steps of 5cm up 50 cm with 10 cm transmitting 4.68E-1 (46.8 %) of the cobalt 60 gamma rays while maximum thickness (50 cm) transmitted fraction of 4.8E-03 (0.48 %).

Determining the half value layer and the tenth value layer for the curve in figure 4.1 it can be seen that the half value layer was about 8.5 cm while the tenth value layer was about 23 cm, as indicated earlier clay and sandstone were found to be almost the same.

The attenuation coefficients were computed for the three materials for different thicknesses and the averages and their deviation. For wood the linear attenuation coefficient (LAC) was 3.76E-02±2.71E-04 cm^{-1} which was lower than for both clay and sandstone. The LACs for clay and sandstone were 8.95E-02±3.19E-03 cm^{-1} and 9.45E-02±3.50E-03 cm^{-1} respectively.

The mass attenuation coefficients (MACs) for wood, clay and sandstone were 5.88E-02±4.24E-04 cm^2g^{-1} ,4.07E-02±1.45E-03 cm^2g^{-1} and 4.07E-02±3.49E-03 cm^2g^{-1} respectively. The relative densities for the three materials contributed to the differencies in the MAC values.

4.2 Cobalt 60 Rectangular plaque Source and Cylindrical source

Results for isotropic point source shown in figure 4.1 and for Rectangular plaque source were almost the same, however due to larger volume of the plaque the values such as HVLs and TVLs were slightly above those of the point source as shown in figure 4.3. The initial thickness (10cm) of wood transmitted 75 % of the initial photon flux as compared to 69.4 % that was transmitted from a point source giving 5.6 % difference. On the other hand for clay 10cm transmitted 54 % for a plaque source while 48.3 % from cobalt 60 point source was transmitted through clay giving the difference of 5.7 % (54 %-48.3 %). Sandstone followed the same behaviour having its 10cm transmitting 52.4 % of gamma rays from cobalt 60 plaque source which was higher by 5.6 % to that transmitted from a point source which was 46.8 %.

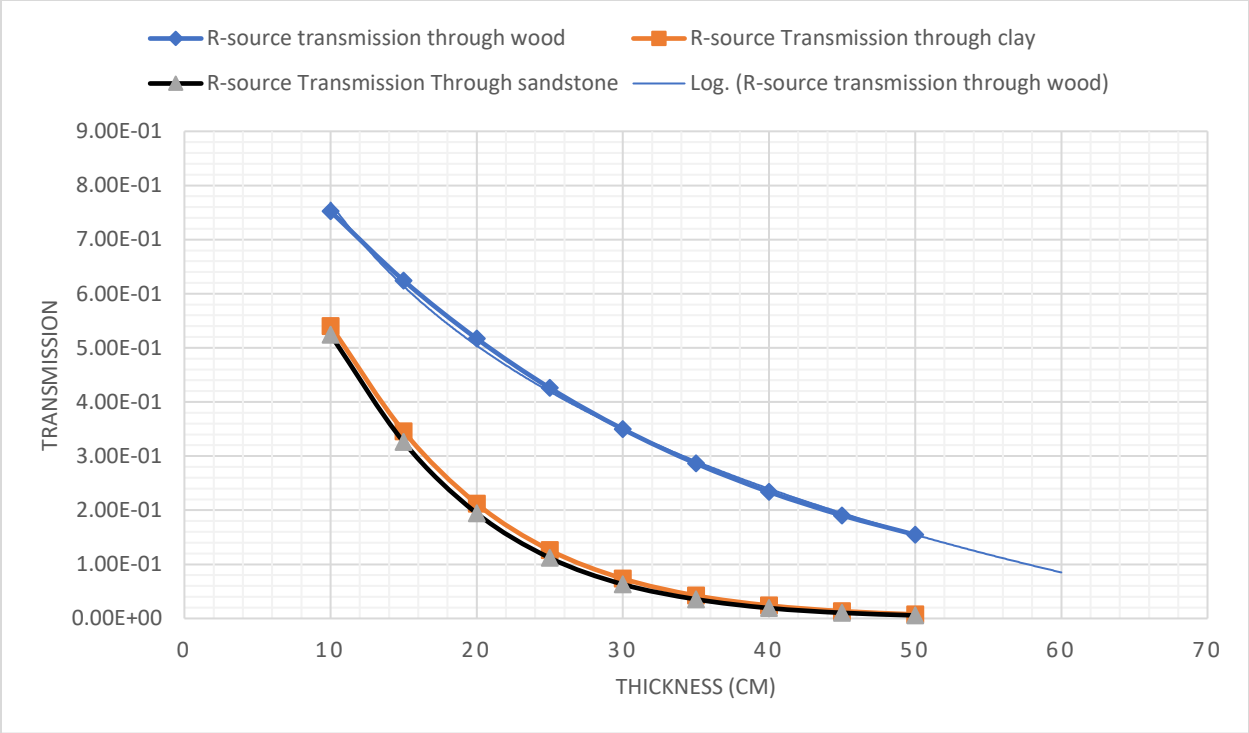

Figure 4.3 : Transmission of cobalt 60 Rectangular plaque source through wood, clay and sandstone.

The HVL for wood in the case of plaque source was found to be 21 cm, 3 cm more than the HVL found for a point source which was 18 cm while the TVL was found to be 57.5 cm for a plaque source 1.5 cm greater than that of a point source which was 56 cm. The difference for TVLs was lower than the difference of HVLs, the thicker the shield, the better it becomes due to an increased probability of interaction and hence better attenuation.

The same happened for clay and sandstone, where clay had a HVL of 11 cm and TVL of 27 cm for plaque source, HVLs differing by 2 cm while TVLs also differed by 2 cm from point source results. For sandstone HVL was 10.5 cm for plaque source being by 2 cm to that of a point source, on the other hand, it was found to be 24.8 cm in the case of plaque

source while it was 23 cm for a point source. Figure 4.4 shows cylindrical source results.

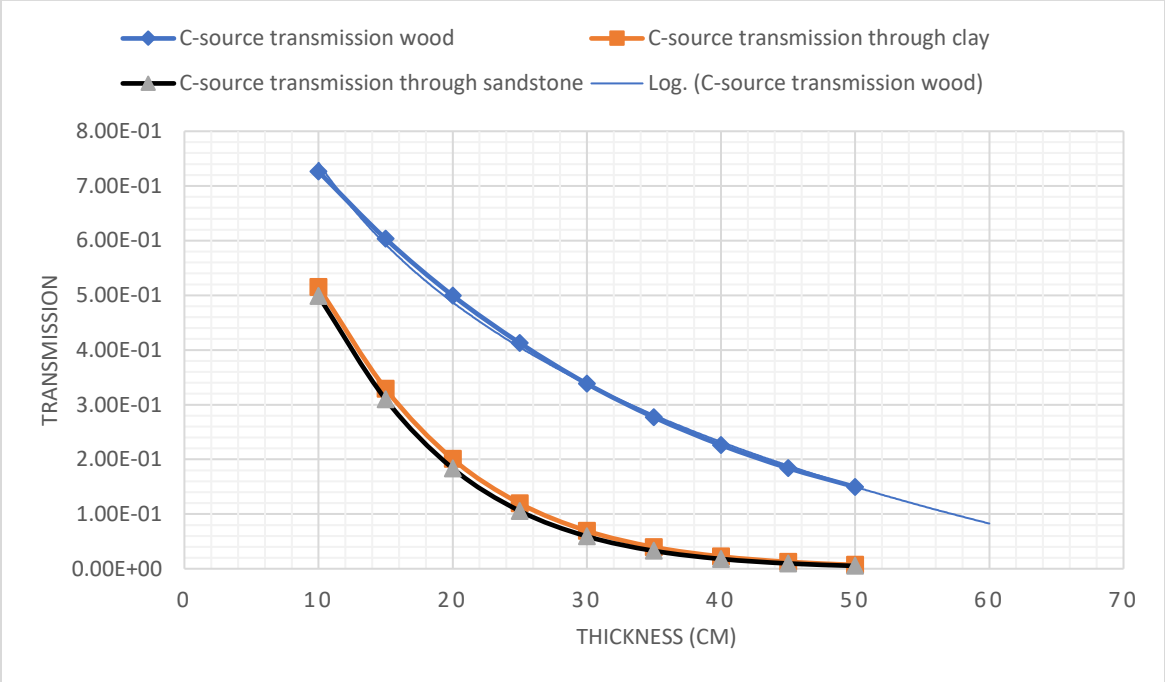

Figure 4.4 : Transmission of cobalt 60 cylindrical sources through wood, clay and sandstone.

The Cylindrical source results were found to fall in between point and plaque sources giving HVLs 20 cm for wood, 10 cm for both clay and sandstone while TVLs was 56.5 cm for wood, 26 cm for clay and 25 cm for sandstone. The three materials were found to be able to lower or reduce flux levels to as low as less than 10 % of the intitial photon flux which can make them good materials to be used as shields for gamma facilities such as the cobalt 60 radiotherapy facility.

4.3 Buildup factors for Cobalt 60 source for wood, clay and sandstone

The ratios of collided photons to uncollided photons known as buildup factors were

computed using point isotropic source and slab shield, the buildup factors were found to increase with the increase in material or shield thickness. The uncollided photon flux was found to decrease as the thickness of the shield increases thus resulting in the increase of the buildup factors.

For wood the factors went up to 2.5 compared to clay and sandstone which went up to 9.00 and 9.84 respectively. The less dense the material is the higher the probability of having uncollided photon flux, the buildup factors are demonstrated in tables 4.3a-c.

4.3a Cobalt- 60 Buildup factors for wood for specified thicknesses

Thickness (cm)	Total photon flux (photons/cm^2)	Uncollided Photon flux (photons/cm^2)	Buildup factors (Total photon flux/Uncollided flux)
10	7.43E-06	5.79E-06	1.28
15	6.17E-06	4.30E-06	1.43
20	5.11E-06	3.22E-06	1.59
25	4.21E-06	2.42E-06	1.74
30	3.46E-06	1.82E-06	1.90
35	2.84E-06	1.38E-06	2.05
40	2.32E-06	1.05E-06	2.21

45	1.89E-06	8.02E-07	2.35
50	1.53E-06	6.14E-07	2.50

4.3b Cobalt- 60 Buildup factors for clay for specified thicknesses

Thickness (cm)	Total photon flux (photons/cm^2)	Uncollided Photon flux (photons/cm^2)	Buildup factors (Total photon flux/Uncollided flux)
10	5.17E-06	2.35E-06	2.20
15	3.29E-06	1.12E-06	2.93
20	2.01E-06	5.39E-07	3.73
25	1.19E-06	2.62E-07	4.53
30	6.88E-07	1.28E-07	5.37
35	3.94E-07	6.31E-08	6.24
40	2.23E-07	3.12E-08	7.14
45	1.25E-07	1.55E-08	8.02
50	6.97E-08	7.74E-09	9.00

4.3c Cobalt- 60 buildup factors for sandstone for specified thicknesses

Thickness (cm)	Total photon flux (photons/cm^2)	Uncollided Photon flux (photons/cm^2)	Buildup factors (Total photon flux/Uncollided flux)
10	5.00355E-06	2.16E-06	2.31

15	3.09046E-06	9.91E-07	3.12
20	1.83406E-06	4.59E-07	4.00
25	1.04575E-06	2.14E-07	4.88
30	5.87777E-07	1.01E-07	5.84
35	3.24142E-07	4.77E-08	6.80
40	1.77078E-07	2.27E-08	7.80
45	9.56805E-08	1.09E-08	8.79
50	5.14079E-08	5.22E-09	9.84

4.4 60 keV,120 keV and 300 keV x-rays transmission through wood

Figure 4.5 shows the dependence of radiation shielding on the energy of x-ray photons. For photons of 60 keV wood is seen to be more effective as compared to shielding of 120 keV photons, the transmission of the two x-ray energies have slight difference at the 5 cm thickness where the difference is 0.04 as compared to wider difference towards the middle of the graph, for instance at 20 cm thickness where the difference in transmission is 0.08. That shows that lower energy photons are easily attenuated than higher energy photons.

To transmit 50 % of 60 keV x-rays using a wood shield, 8 cm thick wood is needed while the 9.5cm thick wood shield is needed to transmit 50 % of 120 keV X-rays and these are HVLs' for wood for the specified X-ray energies according to figure 4.4. The tenth value layers are found to be 24 cm and 30 cm for 60 keV and 120 keV X-rays respectively. The linear attenuation coefficient was found to vary with the energy of the X-rays where it was

found to be 9.12E-2 cm^{-1} (9.12 m^{-1}) ±1.6E-03 for 60 KeV , 7.47E-2 cm^{-1} (7.47 m^{-1})±7.2E-04 for 120 KeV these values lead to MACs being 1.425E-01±8.0E-04 cm^2g^{-1} and 1.17E-01±2.0E-04 cm^2g^{-1} for 60 keV and 120 keV respectively.

Looking at the range 120-300 keV, 120 keV has already been discussed, the 300 keV curve as shown in figure 4.4 behaves the same way as both 60 keV and 120 keV, however, requiring larger thicknesses relative to the two. The half value layer for 300keV was found to be 12.5 cm according to figure 4.4 while the tenth value layer was found to be 36.5 cm and this shows that wood is more effective in shielding lower energy x-rays and thus also justifying the dependence of shielding on the energy of photons attenuated. The computed linear attenuation coefficient was found to be 5.57E-02 cm^{-1} (5.57m^{-1})±5.8E-04 which resulting in MAC being 8.70E-02cm^2g^{-1}. The results were seen to almost agreeing with the results obtained by (Aggrey-Smith et al., 2016) on different species of wood for x-rays ranging from 50-150 KeV , HVLs found were ranging from 15-26 cm for different wood species.

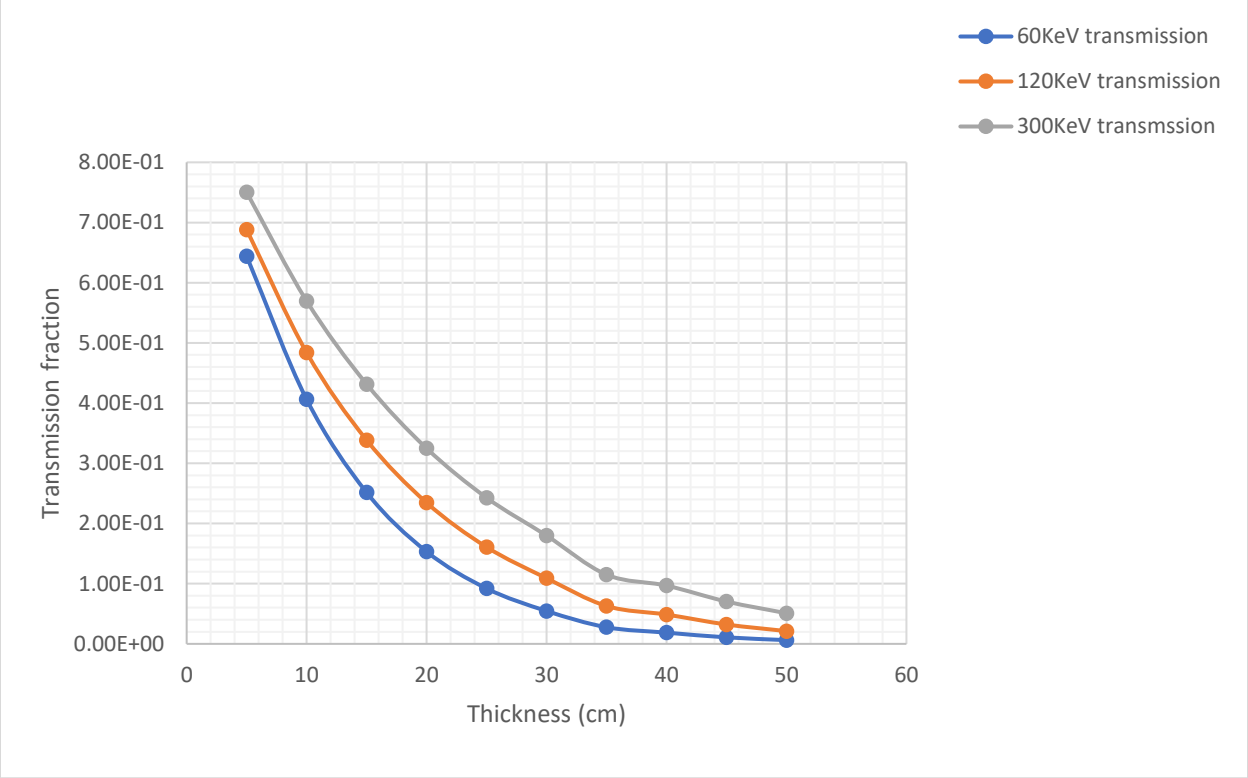

Figure 4.5 Transmission of X-rays of energy 60keV,120keV and 300keV through a slab of wood from 5 cm thickness to 50 cm.

4.5 60 keV, 120 keV and 300 keV x-rays transmission through Clay

Clay is seen to be more effective than wood, the curves in figure 4.5 are more steep as compared to Figure 4.6 the transmission decreases rapidly so much that it starts approaching zero from the thickness of 20 cm and becoming more constant throughout towards 40 cm. what can be seen also is that clay is more effective in shielding low energy photons, this can be seen on the blue 60keV curve which decreases sharply almost making

a sharp corner at the thickness of 5 cm before almost becoming constant through to 40cm as compared to 120 keV and 300 keV curves. For 60 keV x-rays the LAC was found to be 5.74E-01 cm^{-1} with the deviation of ± 2.0E-02 and MAC was 2.61E-01±3.2E-04 cm^2g^{-1}.

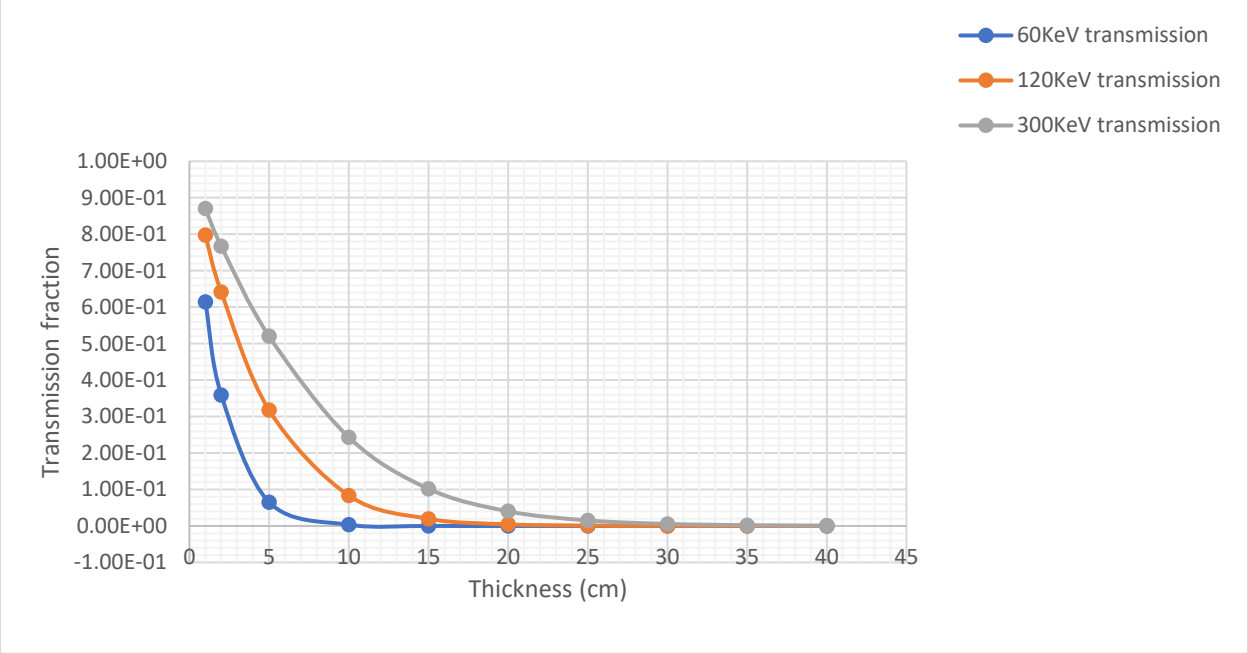

Figure 4.6 Transmission of X-rays of energy 60 keV,120 keV and 300 keV through slab of clay from 1 cm thickness to 40 cm.

For 120 keV and 300 keV LACs were found to be (2.6E-01±9.0E-03) and (1.56E-01±6.0E-03) cm^{-1} respectively, while MACs were 1.18E-01±4.0E-05 cm^2g^{-1} and 7.09E-02±6.1E-04 cm^2g^{-1} for 120 keV and 300 keV respectively. The photons attenuated per unit length for clay are more than those attenuated per unit length of wood for all energies make clay a

better shield than wood. The HVL of clay for 60 KeV according to figure 4.5 is 1.5 cm which far less than HVL of wood which was found to 8 cm making a more efficient shield than wood also comparing their TVLs' which was found to be 4.3 cm for clay still on 60 keV photons while it was found to be 24 cm for wood.

The HVLs' for 120 keV and 300 keV for clay according to figure 4.6 are 3cm and and 5.5 cm respectively, still this values show that clay is a better shield because it needs a far less thickness to provide same protection compared to 9.5 and 12.5 cm being the HVLs' of wood for 120 keV and 300 keV X-rays respectively. The TVLs' give same analogy as the HVLs' where clay was found to have a TVL of 9.5 cm for 120 keV and 15 cm for 300 keV while it was found to be 30cm for 120 keV and 36.5 cm 300 keV for wood.

4.6 60 keV, 120 keV and 300 keV x-rays transmission through sandstone

As it can be seen from figure 4.6 the curves display the same behaviour as the curve in figure 4.5, hence the results for clay compare almost the same way as they did for cobalt 60 gamma source with the 60keV descending more rapidly than the both 120keV and 300keV as the lesser energy photons are likely to interact with the shield, the higher the energy of the photon the more penetrating it becomes. The higher energy of Cobalt 60 photons showed thicker HVLs and TVLs and low LACs as compared to x-rays.

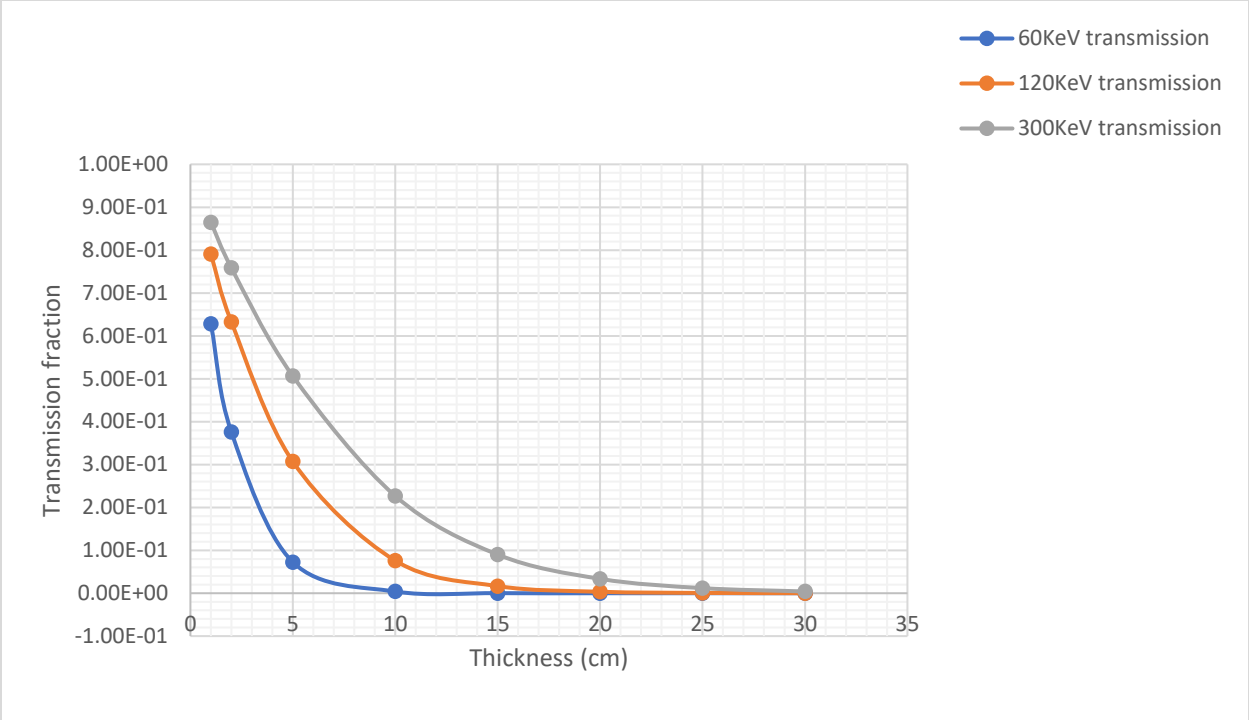

Figure 4.7 The transmission of X-rays of energy 60 keV, 120 keV and 300 keV through a slab of sandstone from 1 cm thickness to 30 cm.

From Figure 4.7, sandstone had HVLs 1.2 cm for 60 keV, 3 cm for 120 keV and 5 cm for 300 keV. The TVLs was 4.5 cm for 60 keV, 9.2 cm for 120 keV and 14 cm for 300 keV. The LACs were for to be 5.40E-01±1.5E-02 cm^{-1} for 60 keV, 2.63E-01±9.7E-03 cm^{-1} for 120 keV and 1.57E-01±7.0E-03 cm^{-1} for 300 keV, all the three values compare perfectly with the values for clay although clay was found have slightly better LACs. This can be due to the fact that LAC does not depend only on density but also other parameters such as chemical composition, mechanical and physical properties hence even though clay had a slightly lower density than sandstone it is found to have better LACs.

Due to their comparable densities, with clay having 2.20 g/cm^3 and sandstone having 2.32 g/cm^3, the attenuation per unit length is justifiable or foreseeable to be comparable. The MACs for different x-ray energies were found to be 2.33E-01±6.5E-03 cm^{2}g^{-1} for 60 keV, 1.13E-01±4.2E-03 cm^{2}g^{-1} for 120 keV and 6.93E-02±2.8E-03 cm^{2}g^{-1} for 300 keV. The better shield is regarded as the one with higher density and low HVL, clay and sandstone were seen to be better than wood, with the two being almost the same. The three materials showed that they can all provide protection in x-rays facilities , especially diagnostic X-rays facilities since they were able to reduce radiation levels as low as 10^{-13} as shown in Figures 4.5-4.7

4.7 Buildup factors for x-rays

The buildup factors for different x-rays energies are shown in Tables 4.7. They also display the same behavior as the factors for cobalt 60 increasing with an increase in the material or shield thickness. In case of x-rays have values higher than 30 for clay irradiated with 120 keV x-rays, this can be due to lower values of uncollided photons since x-rays used had lower energies than energies of gamma particles from cobalt-60 (with energies 1.17 and 1.33 MeV) thus being less penetrating. Cobalt-60 buildup factors are shown in section 4.6.

4.7a 60 keV X-rays buildup factors for wood for specified thicknesses

thickness(cm)	Total photon flux (photons/cm^2)	Uncollided Photon flux (photons/cm^2)	Buildup factors (Total photon flux/Uncollided flux)
5	6.63E-06	4.88E-06	1.36

10	4.18E-06	2.3E-06	1.82
15	2.59E-06	1.09E-06	2.37
20	1.58E-06	5.24E-07	3.01
25	9.48E-07	2.54E-07	3.74
30	5.62E-07	1.24E-07	4.55
35	2.85E-07	5.66E-08	5.03
40	1.92E-07	2.98E-08	6.44
45	1.11E-07	1.48E-08	7.54
50	6.39E-08	7.34E-09	8.70

4.7b 120 keV X-rays buildup factors for wood for specified thicknesses

thickness(cm)	Total photon flux (photons/cm^2)	Uncollided Photon flux (photons/cm^2)	Buildup factors (Total photon flux/Uncollided flux)
5	7.36E-06	5.63E-06	1.31
10	5.18E-06	3.04E-06	1.71
15	3.62E-06	1.65E-06	2.19
20	2.51E-06	9.07E-07	2.77
25	1.72E-06	5.02E-07	3.43
30	1.17E-06	2.79E-07	4.18
35	6.73E-07	1.46E-07	4.62

40	5.21E-07	8.77E-08	5.93
45	3.44E-07	4.95E-08	6.95
50	2.26E-07	2.8E-08	8.07

4.7c 300 keV X-rays buildup factors for wood for specified thicknesses

thickness(cm)	Total photon flux (photons/cm^2)	Uncollided Photon flux (photons/cm^2)	Buildup factors (Total photon flux/Uncollided flux)
5	8.03E-06	6.49E-06	1.24
10	6.09E-06	4.01E-06	1.52
15	4.62E-06	2.50E-06	1.85
20	3.48E-06	1.57E-06	2.22
25	2.6E-06	9.89E-07	2.63
30	1.93E-06	6.28E-07	3.07
35	1.23E-06	3.72E-07	3.30
40	1.04E-06	2.56E-07	4.04
45	7.52E-07	1.65E-07	4.56
50	5.44E-07	1.06E-07	5.12

4.7d 60 keV X-rays Buildup factors for clay for specified thicknesses

thickness(cm)	Total photon flux (photons/cm^2)	Uncollided Photon flux (photons/cm^2)	Buildup factors (Total photon flux/Uncollided flux)
1	6.33E-06	5.10E-06	1.24
2	3.7E-06	2.48E-06	1.49
5	6.73E-07	2.88E-07	2.33
10	3.42E-08	8.32E-09	4.10
15	1.66E-09	2.51E-10	6.61
20	9.02E-11	7.78E-12	11.59
25	5.42E-12	2.48E-13	21.84
30	1.12E-13	8.09E-15	13.89
35	2.81E-15	2.68E-16	10.47
40	7.43E-17	9.02E-18	8.23

4.7e 120 keV X-rays Buildup factors for clay for specified thicknesses

thickness(cm)	Total photon flux (photons/cm^2)	Uncollided Photon flux (photons/cm^2)	Buildup factors (Total photon flux/Uncollided flux)
1	8.53E-06	7.10E-06	1.20
2	6.86E-06	4.78E-06	1.43
5	3.4E-06	1.47E-06	2.31

10	8.94E-07	2.11E-07	4.23
15	2.1E-07	3.11E-08	6.77
20	4.69E-08	4.65E-09	10.07
25	1.01E-08	7.08E-10	14.24
30	2.08E-09	1.09E-10	19.04
35	4.39E-10	1.70E-11	25.76
40	9.18E-11	2.68E-12	34.32

4.7f 300 keV X-rays Buildup factors for clay for specified thicknesses

thickness(cm)	Total photon flux (photons/cm^2)	Uncollided Photon flux (photons/cm^2)	Buildup factors (Total photon flux/Uncollided flux)
1	9.31E-06	8.06E-06	1.16
2	8.21E-06	6.13E-06	1.34
5	5.57E-06	2.72E-06	2.05
10	2.6E-06	7.10E-07	3.66
15	1.09E-06	1.89E-07	5.77
20	4.29E-07	5.10E-08	8.42
25	1.63E-07	1.39E-08	11.68
30	5.96E-08	3.84E-09	15.52
35	2.14E-08	1.07E-09	20.05
40	7.6E-09	2.99E-10	25.38

4.7g 60 keV X-rays Buildup factors for sandstone for specified thicknesses

Thickness(cm)	Total photon flux (photons/cm^2)	Uncollided Photon flux (photons/cm^2)	Buildup factors (Total photon flux/Uncollided flux)
1	6.47E-06	5.15E-06	1.26
2	3.87E-06	2.52E-06	1.53
5	7.48E-07	3.02E-07	2.47
10	4.12E-08	9.15E-09	4.50
15	2.09E-09	2.89E-10	7.24
20	9.89E-11	9.38E-12	10.54
25	6.4E-12	3.13E-13	20.43
30	3.59E-13	1.07E-14	33.65

4.7h 120 keV X-rays Buildup factors for sandstone for specified thicknesses

Thickness(cm)	Total photon flux (photons/cm^2)	Uncollided Photon flux (photons/cm^2)	Buildup factors (Total photon flux/Uncollided flux)
1	8.46392E-06	6.96E-06	1.22
2	6.77153E-06	4.59E-06	1.48
5	3.28423E-06	1.33E-06	2.48
10	8.13294E-07	1.72E-07	4.74

15	1.77987E-07	2.28E-08	7.82
20	3.69255E-08	3.08E-09	11.98
25	7.33515E-09	4.25E-10	17.28
30	1.38343E-09	5.92E-11	23.35

4.7i 300 keV X-rays Buildup factors for sandstone for specified thicknesses

Thickness(cm)	Total photon flux (photons/cm^2)	Uncollided Photon flux (photons/cm^2)	Buildup factors (Total photon flux/Uncollided flux)
1	9.25306E-06	7.94E-06	1.17
2	8.11871E-06	5.94E-06	1.37
5	5.4166E-06	2.51E-06	2.16
10	2.42672E-06	6.08E-07	3.99
15	9.64061E-07	1.50E-07	6.43
20	3.58499E-07	3.75E-08	9.55
25	1.27079E-07	9.51E-09	13.37
30	4.38626E-08	2.43E-09	18.02

4.8 Cost-Benefit Analysis and optimization analysis of the materials

The simple rectangular plane was considered as a shield in the analysis, which can be said to be a wall for a room directly from the radiation source. The controlling parameter for cost and optimization was the thickness of the shielding material, other parameters such as

cost of installation, cost of production and were assumed based on materials from Lesotho. Some other parameters were computed from results obtained, such as effective attenuation coefficients (r), number of HVLs required to reduce cobalt 60 gamma source to 1mSv/year in agreement with (NCRP 116, 1994).

The effective dose at the face of the initial thickness (H_u) was assumed to be 0.034Sv/year at 100 cm as indicated in ☻ (Delacroix, Guerre, Leblanc, & Hickman, 2002), thus the number of HVLs was found to be 5.1HVLs. This implied that the minimum thickness required for wood was 91 cm (0.91 m) since the HVL of wood was found to be 18 cm, 45.9 cm (0.46 m) for clay whose thickness was found to be 9 cm and 43.35 cm (0.43 m) for sandstone where the HVL was found to 8.5 cm. If the lead shield was to be used, the minimum thickness required would be 7.65 cm (0.0765 m) since its HVL was found to be 1.5 cm. The result shows that the minimum thickness required for sandstone is less than that would be required for both clay and wood. Effective attenuation coefficient calculated using computed buildup factors for each material were; 5.3 m^{-1} for wood, 12.3 m^{-1} for clay and 13 m^{-1} for sandstone. Optimized dose reduction factors (e^{-rw}) were computed using equation (17). The costs were assumed based on the average costs of each material in Lesotho and were fixed for each material. The assumed cost of installation for a square plane shield with dimensions 9 m x 9 m for wood was \$80/m^3.

The dimensional constant α expressing cost assigned to the unit collective dose was assumed to be \$1000 $(manSv)^{-1}$ which was fixed for all materials, ρ = 1, time for installations is mostly assumed to be from 20-50 years, minimum was taken, thus $\tau = 20\ years$. For workers it was assumed that one person was exposed in 6 m^2, that is 6 m^2/man. The dose reduction factor for wood was found to be 0.083, which means for wood

the objective in design should be to reduce dose by a factor of 8.3. The dose reduction factors were 0.06 and 0.07 for clay and sandstone respectively, the costs of installation for clay, assumed to be \$80/m^3 while it was assumed to \$100/m^3 for sandstone.

The net cost benefit B_s was calculated for each of the three materials where the gross benefit V was assumed to be \$10000 which the assumed cost which would be saved if another material was to be used instead of lead. Prior to calculations of Benefits, X(w) which is the cost of achieving the required radiation protection was calculated using equation (16) where the cost of support installation was assumed to be \$750 and fixed for the three materials. X(w) which depends on thickness w was found to \$4395 for wood, while it was \$3730.8 and \$4233 for clay and sandstone respectively. Y(w) which costs of detriment was also calculated using equation (14) which also depend on thickness w, Y(w)s were found to be \$338.64 for wood, \$244.80 for clay and \$285.6 for sandstone.

The net cost benefit B_s was found to be positive for all the three materials, the value for wood was \$4266.36 for wood where the cost of production P for wood was assumed to \$1000. For clay B_s was found to \$4224.40 and P was to be \$1500 for clay. For sandstone the B_s was found to be \$4481.4 with P assumed to be \$1000. It was found to be more beneficial to use wood for all the three materials in terms of cost, however, the required thickness for wood is huge almost one-meter thick shield thus wood can opt if x-rays with lower energies are used. The most optimum thickness can be for sandstone for cobalt 60 since 0.43 m was required, however, it was not too different from minimum thickness required for clay which was 0.46 m.

CHAPTER FIVE

5.1 Conclusions and recommendations

The analysis for the effectiveness of wood, clay and sandstone was done using the MCNP code, results were interpreted and computations of other radiation shielding parameters were done based on literature alongside with cost-benefit analysis. The transmitted photon flux estimated for each of the three materials for gamma source (cobalt- 60) and x-rays of enegies ranging from 60-300 keV. All the three materials were found to be effective for all radiation sources used since they were able to lower the photons flux below 10 % for thicknesses beyond 57 cm for ^{60}Co and 36.5 cm for X-rays.

Clay and sand sandstone were more effective for cobalt 60 since the required thicknesses were far lower than 0.91 m required for wood thus in terms of more favourable thickness clay and sandstone were better materials to opt for in protection against cobalt 60. For x-rays also it was found that all materials were able to reduce photon flux within 10^{-13}-10^{-9} photons/cm^2. In this study, cost-benefit was done, most monetary values were assumed since the installation has not been done for the materials used, assumptions were made based on the cost of the materials in Lesotho. The values of benefit B_s were all positive showing that the practice can be done.

In terms of cost, all materials were found to be cheaper relative to lead. For favourable thicknesses, for cobalt-60 (1MBq and exposure rate of 0.034 Sv/y at 100 cm distance (Delacroix et al., 2002)) source the thickness of 0.91 m was required for wood, which can be difficult to install considering the nature of wood.

For x-rays however, all materials had favourable thicknesses though wood can be prefered

for lower energy x-rays for diagnostic X-ray facilities since it was found that 24 cm thick wood transmits 10 % of 60 keV energy x-rays and 30 cm transmits 10 % of 120 keV energy x-rays.

The minimum thickness required to transmit 10 % of 300 keV x-rays for wood was 36.5 cm which was better than Tenth Value Layer (TVL) required for cobalt 60 hence it can be concluded that wood was a better protection for x-rays than cobalt 60 source in terms of optimum shield, in the same way, it can be concluded that clay and sandstone were also better shield for x-rays than cobalt 60 since for the highest x-rays energy used in this study, that is 300 keV, TVLs computed were 14 cm and 15 cm for clay and sandstone respectively.

These were all less than thicknesses computed for shielding gamma radiation which were 43 cm and 46 cm for sandstone and clay respectively. The results were all compared to lead in (F.S Kirn 1954) and those that were computed in this study, although lead is a better shield in terms of very low required thicknesses for radiation protection, in terms of cost, wood, clay and sandstone can be options since they were all found to be effective for radiation shielding of plaque, point and cylindrical source geometries and collimated x-ray sources. However, materials need to be carefully prepared to minimize the number of voids and maintain homogeneity to avoid radiation leakages.

5.2 Recommendations

From the findings of the study carried on clay, wood and sandstone, the following recommendations are made to:

I. Facilities and Activities

- To improve the application of radiation technology as low cost; wood, clay and sandstone can be used in radiation protection for shielding if a qualified radiation protection specialist guides in the installations.
- Sandstone is highly recommended specifically for higher energy radiations such as gamma rays in cobalt 60 radiotherapy facilities, as it found in a ready solid form compared to clay which may need to be converted into ceramic form and thickness required is not very large compared to wood.
- For lower energy x-rays especially in medical facilities, all materials (clay, wood and sandstone) can be better options.

II. Regulatory Authority

- The installations can be frequently checked at least every six months by radiation protection specialits for monitoring the doses incurred by exposed personnel including the public.

III. Research Institutions

- In future, further research on clay, wood and sandstone can be done to investigate the effectiveness of these materials in shielding neutrons.
- In future, same analysis on wood, clay and sandstone can be done experimentally and compare the results with MCNP results.

REFERENCES

Aggrey-Smith, S., Preko, K., W. Owusu, F., & K. Amoako, J. (2016). Study of Radiation Shielding Properties of selected Tropical Wood Species for X-rays in the 50-150 keV Range. *The Open Access Journal of Science and Technology*, *4*. https://doi.org/10.11131/2016/101150

Alrammah, I. A. (2016). Application of MCNP Code in Shielding Design for Radioactive Sources, *4*(1).

Brown, F. B., & Martin, W. R. (1984). MONTE CARLO METHODS FOR RADIATION TRANSPORT ANALYSIS ON VECTOR COMPUTERS, *14*(3).

Cacuci, D. G. (2010). Handbook of Nuclear Engineering (Volume I Nuclear Engineering Fundamentals). *Springer*, 3642.

Chawla, K. (2013). Material Characterization Techniques, 1–9.

Chen, C., & Wang, M. (2011). The Optimization of Material Thickness for Neutron Shielding With Monte Carlo Method, *142*, 166–169. https://doi.org/10.4028/www.scientific.net/AMR.142.166

Coderre P. (2006). The History of the Discovery of Radiation and Radioactivity, 1–11.

Peter J. Biggs. (2014). Radiation Shielding for Megavoltage Photon Therapy Machines.

Data, E. (2011). X- and γ-radiation. *IARC Monographs on the Evaluation of*

Carcinogenic Risks to Humans, *100 D*, 103–229.

Davraz, M., Pehlivanoğlu, H. E., Kilinçarslan, Ş., & Akkurt, İ. (2017). Determination of Radiation Shielding of Concrete Produced from Portland Cement with Boron Additives, *132*(3), 702–704. https://doi.org/10.12693/APhysPolA.132.702

Delacroix, D., Guerre, J. P., Leblanc, P., & Hickman, C. (2002). AND RADIATION PROTECTION DATA HANDBOOK 2002, *98*(1).

Environmental Health and Safety's Radiation Control office, U. of F. (n.d.). Rssc radiation protection 07/11 3-1. *Chapter 3 Radiation Protection*, 1–52. Retrieved from http://webfiles.ehs.ufl.edu/rssc_stdy_chp_3.pdf

International Atomic Energy Agency. (2001). IAEA-TECDOC-1191: Categorization of radiation sources, (March). Retrieved from http://www-pub.iaea.org/MTCD/Publications/PDF/te_1191_prn.pdf

Kafi, A. Al, Maalej, N., & Naqvi, A. A. (2005). THE USE OF MCNP CODE FOR RADIATION TRANSPORT AND DOSIMETRY CALCULATIONS IN TRAINING MEDICAL PHYSICS STUDENTS Abdullah Al Kafi , Nabil Maalej , Akhtar Abbas Naqvi , *15*, 1–5.

Kleijnen, J. P. C., Ridder, A. A. N., & Rubinstein, R. Y. (2010). Variance Reduction Techniques in Monte Carlo Methods, *3*(1), 1–17.

Koddenberg, T. (2016). *Handbook of Wood Chemistry and Wood Composites*. *Journal of Cleaner Production* (Vol. 110). https://doi.org/10.1016/j.jclepro.2015.07.070

Lištjak, M. M., Ondrej, R. O. S., Kubovi, I. D., & Vermeersch, F. (2008). Buildup factors

for Multilayer shieldings in Deterministic methods and their comparison with Monte Carlo, 2–5.

McConn, R. J., Gesh, C. J., Pagh, R. T., Rucker, R. A., & Williams III, R. (2011). Compendium of Material Composition Data for Radiation Transport Modeling. https://doi.org/10.2172/1023125

Morad, S. R. H. Worden (2000.). *Quartz Cementation in Sandstones*. Blackwell science

Morari, G. (2016). *Clays, Clay Minerals and Ceramic Materials Based on Clay Minerals*. pub-ExLi4EvA

Nelson, G., & Rewy, D. (1909). Gamma Interaction with Matter, (I).

Pettersen, R. C. (1984). The Chemical Composition of Wood. *U.S. Department of Agriculture, Forest Service, Forest Products Laboratory, Madison, WI 53705*, 70. https://doi.org/10.1021/ba-1984-0207.ch002

Reilly, D., Ensslin, N., H., S., & Kreiner, S. (1991). The Origin Gamma Rays. *Passive Nondestructive Assay of Nuclear Materials*, 1–25. https://doi.org/10.1098/rspa.1931.0125

Shultis, J. K., & Faw, R. E. (1979). RADIATION SHIELDING TECHNOLOGY. Vol-88

Taylor, P. & Francis (2012). Journal of Nuclear Science and Technology, A Monte Carlo Method For Radiation Transport Calculation, 37–41. https://doi.org/10.1080/18811248.1972.9734896

Thomas E. Johnson, Herman Cember (2008). Introduction to Health Physics. 4th Edition

US NRC: Uses of Radiation. (2014). Retrieved from http://www.nrc.gov/about-

nrc/radiation/around-us/uses-radiation.html

L.V Spencer, U Fano. (1951) Penetration and Diffusion of X-rays. Calculation of spatial Distribution by Polynomial Expansion.

Glenn F. Knoll. (2010). Radiation Detection and measurement, 3rd edition.

Y. Harima. (1983). An approximation of Gamma-Ray Buildup factors by modified geometrical progression, Vol 3

Y Harima. (1986). Validity of the geometric-progession formula in Approximating Gamma-Ray, Volume 83.

International Commission on Radiological Protection (ICRP), (1983). Cost-Benefit Analysis in the optimization of radiation protection, Vol 10.

Dimitris S. Gorpas, Stefan Andersson-Engels. (2012). Evaluation of a Radiative transfer equation and diffusion approximation hybrid forward solver for fluorescence molecular imaging. journal of biomedical optics 17 (12)

Simmons SL, (1973). An adjoint Gamma-Ray Moments Computer Code, ADJMOM-I

APPENDICES

Appendix A

Table A1: Chemical composition of wood in MCNP form for photons (McConn et al., 2011).

Weight Fractions	Atom Fractions	Atom Densities	Weight Fractions	Atom Fractions	Atom Densities
1000	-0.059642	1000	0.462423	1000	0.022806
6000	-0.497018	6000	0.323389	6000	0.015949
7000	-0.004970	7000	0.002773	7000	0.000137
8000	-0.427435	8000	0.208779	8000	0.010297
12000	-0.001988	12000	0.000639	12000	0.000032
16000	-0.004970	16000	0.001211	16000	0.000060
19000	-0.001988	19000	0.000397	19000	0.000020
20000	-0.001988	20000	0.000388	20000	0.000019

Table A2: Chemical composition of clay in MCNP form for photons(McConn et al., 2011).

Weight Fractions	Atom Fractions	Atom Densities	Weight Fractions	Atom Fractions	Atom Densities
8000	-0.484345	8000	0.633300	8000	0.040107
11000	-0.007608	11000	0.006923	11000	0.000438
12000	-0.010691	12000	0.009202	12000	0.000583
13000	-0.122125	13000	0.094689	13000	0.005997
14000	-0.294194	14000	0.219134	14000	0.013878
15000	-0.000113	15000	0.000076	15000	0.000005
19000	-0.020427	19000	0.010930	19000	0.000692
20000	-0.018957	20000	0.009895	20000	0.000627
22000	-0.004668	22000	0.002040	22000	0.000129
25000	-0.000064	25000	0.000024	25000	0.000002
26000	-0.036804	26000	0.013787	26000	0.000873

Table A3: Chemical composition of sandstone in MCNP form for photons(McConn et al., 2011).

Weight Fractions	Atom Fractions	Atom Densities	Weight Fractions	Atom Fractions	Atom Densities
1000	-0.001791	1000	0.034647	1000	0.002483
6000	-0.013652	6000	0.022161	6000	0.001588
8000	-0.519609	8000	0.633160	8000	0.045375
11000	-0.002969	11000	0.002518	11000	0.000180
12000	-0.007240	12000	0.005807	12000	0.000416
13000	-0.025417	13000	0.018365	13000	0.001316
14000	-0.366185	14000	0.254190	14000	0.018216
16000	-0.000280	16000	0.000171	16000	0.000012
19000	-0.011628	19000	0.005798	19000	0.000416
20000	-0.039328	20000	0.019131	20000	0.001371
22000	-0.001199	22000	0.000488	22000	0.000035
26000	-0.010031	26000	0.003502	26000	0.000251
82000	-0.000671	82000	0.000063	82000	0.000005

Appendix B

Table B1: The detected photon flux from cobalt 60 point source beyond wood shield for respective thicknesses and the transmission.

Thickness (cm)	flux at point 1 (photons/cm^2)	flux at point 2 (photons/cm^2)	flux Average, photons/cm^2	transmission through wood
10	7.62E-06	7.24E-06	7.42567E-06	6.94E-01
15	6.31E-06	6.03E-06	6.16648E-06	5.76E-01
20	5.21E-06	5.00E-06	5.1072E-06	4.77E-01
25	4.29E-06	4.13E-06	4.21032E-06	3.93E-01
30	3.53E-06	3.40E-06	3.46371E-06	3.24E-01
35	2.88E-06	2.79E-06	2.83702E-06	2.65E-01
40	2.35E-06	2.28E-06	2.3177E-06	2.17E-01
45	1.91E-06	1.86E-06	1.88824E-06	1.76E-01
50	1.56E-06	1.51E-06	1.53435E-06	1.43E-01

Table B2: The detected photon flux from cobalt 60 point source beyond clay shield for respective thicknesses and the transmission.

Thickness (cm)	flux at point 1 (photons/cm^2)	Flux at point 2 (photons/cm^2)	Average photon flux (Photons/cm^2)	Transmission through clay
10	5.32E-06	5.02E-06	5.17E-06	4.83E-01
15	3.19E-06	3.38E-06	3.29E-06	3.07E-01
20	2.07E-06	1.95E-06	2.01E-06	1.88E-01
25	1.22E-06	1.15E-06	1.19E-06	1.11E-01
30	7.08E-07	6.68E-07	6.88E-07	6.43E-02
35	4.05E-07	3.82E-07	3.94E-07	3.68E-02
40	2.29E-07	2.17E-07	2.23E-07	2.09E-02
45	1.28E-07	1.21E-07	1.25E-07	1.16E-02
50	7.15E-08	6.79E-08	6.97E-08	6.51E-03

Table B3: The detected photon flux from cobalt 60 point-source beyond sandstone shield for respective thicknesses and the transmission.

Thickness (cm)	Flux at point 1 (photons/cm^2)	Flux at point 2 (photons/cm^2)	Average photons/cm^2	transmission through sandstone
10	5.15E-06	4.86E-06	5.00E-06	4.68E-01
15	3.18E-06	3.00E-06	3.09E-06	2.89E-01
20	1.89E-06	1.77E-06	1.83E-06	1.71E-01
25	1.08E-06	1.01E-06	1.05E-06	9.77E-02
30	6.05E-07	5.70E-07	5.88E-07	5.49E-02
35	3.34E-07	3.15E-07	3.24E-07	3.03E-02
40	1.82E-07	1.72E-07	1.77E-07	1.65E-02
45	9.86E-08	9.28E-08	9.57E-08	8.94E-03
50	5.29E-08	4.99E-08	5.14E-08	4.80E-03

Table B4: The detected photon flux from cobalt 60 cylindrical source beyond wood shield for respective thicknesses and the transmission.

thickness (cm)	Flux at point 1 (photons/cm^2)	Flux at point 2 (photons/cm^2)	Average flux (photons/cm^2)	Transmission (photons/cm^2)
10	7.66E-06	7.88E-06	7.77E-06	7.26E-01
15	6.55E-06	6.37E-06	6.46E-06	6.03E-01
20	5.28E-06	5.41E-06	5.34E-06	5.00E-01
25	4.48E-06	4.36E-06	4.42E-06	4.13E-01
30	3.66E-06	3.58E-06	3.62E-06	3.38E-01
35	3.00E-06	2.93E-06	2.96E-06	2.77E-01
40	2.45E-06	2.40E-06	2.42E-06	2.26E-01
45	1.99E-06	1.95E-06	1.97E-06	1.84E-01
50	1.62E-06	1.59E-06	1.60E-06	1.50E-01

Table B5: The detected photon flux from cobalt 60 cylindrical source beyond clay shield for respective thicknesses and the transmission.

thickness (cm)	Flux at point 1 (photons/cm^2)	Flux at point 2 (photons/cm^2)	Average flux (photons/cm^2)	transmission through clay
10	5.61E-06	5.41E-06	5.51E-06	5.15E-01
15	3.58E-06	3.45E-06	3.52E-06	3.29E-01
20	2.10E-06	2.19E-06	2.15E-06	2.01E-01
25	1.30E-06	1.25E-06	1.28E-06	1.19E-01
30	7.57E-07	7.27E-07	7.42E-07	6.93E-02
35	4.33E-07	4.15E-07	4.24E-07	3.97E-02
40	2.45E-07	2.35E-07	2.40E-07	2.25E-02
45	1.37E-07	1.32E-07	1.35E-07	1.26E-02
50	7.65E-08	7.35E-08	7.50E-08	7.01E-03

Table B6: The detected photon flux from cobalt 60 cylindrical source beyond sandstone shield for respective thicknesses and the transmission.

thickness (cm)	Flux at point 1(photons/cm^2)	Flux at point 2 (photons/cm^2)	Average flux (photons/cm^2)	transmission through sandstone
10	5.43E-06	5.24E-06	5.34E-06	4.99E-01
15	3.38E-06	3.25E-06	3.31E-06	3.10E-01
20	2.00E-06	1.92E-06	1.96E-06	1.83E-01
25	1.15E-06	1.11E-06	1.13E-06	1.06E-01
30	6.47E-07	6.21E-07	6.34E-07	5.93E-02
35	3.57E-07	3.43E-07	3.50E-07	3.27E-02
40	1.96E-07	1.88E-07	1.92E-07	1.79E-02
45	1.06E-07	1.01E-07	1.03E-07	9.67E-03
50	5.72E-08	5.47E-08	5.60E-08	5.23E-03

Table B7: The detected photon flux from cobalt 60 plaque source beyond wood shield for respective thicknesses and the transmission.

Thickness (cm)	Flux at point 1 (photons/cm^2)	Flux at point 2 (photons/cm^2)	Average flux (photons/cm^2)	transmission through wood
10	8.08E-06	8.01E-06	8.05E-06	7.52E-01
15	6.72E-06	6.65E-06	6.68E-06	6.24E-01
20	5.57E-06	5.50E-06	5.53E-06	5.17E-01
25	4.53E-06	4.58E-06	4.56E-06	4.26E-01
30	3.72E-06	3.77E-06	3.74E-06	3.50E-01
35	3.08E-06	3.04E-06	3.06E-06	2.86E-01
40	2.52E-06	2.48E-06	2.50E-06	2.34E-01
45	2.02E-06	2.05E-06	2.04E-06	1.90E-01
50	1.67E-06	1.64E-06	1.65E-06	1.55E-01

Table B8: The detected photon flux from cobalt 60 plaque source beyond clay shield for respective thicknesses and the transmission.

Thickness (cm)	Flux at point 1 (photons/cm^2)	Flux at point 2 (photons/cm^2)	Average flux photons/cm^2	Transmission through clay
10	5.83E-06	5.73E-06	5.78E-06	5.40E-01
15	3.74E-06	3.66E-06	3.70E-06	3.46E-01
20	2.29E-06	2.24E-06	2.27E-06	2.12E-01
25	1.36E-06	1.33E-06	1.35E-06	1.26E-01
30	7.98E-07	7.77E-07	7.87E-07	7.36E-02
35	4.57E-07	4.46E-07	4.52E-07	4.22E-02
40	2.59E-07	2.53E-07	2.56E-07	2.39E-02
45	1.46E-07	1.42E-07	1.44E-07	1.34E-02
50	8.09E-08	7.91E-08	8.00E-08	7.48E-03

Table B9: The detected photon flux from cobalt 60 plaque source beyond sandstone shield for respective thicknesses and the transmission.

Thickness (cm)	stone a	Flux at point 2 (photons/cm^2)	Average flux (photons/cm^2)	Transmission Through sandstone
10	5.66E-06	5.56E-06	5.61E-06	5.24E-01
15	3.45E-06	3.52E-06	3.49E-06	3.26E-01
20	2.10E-06	2.06E-06	2.08E-06	1.94E-01
25	1.21E-06	1.18E-06	1.20E-06	1.12E-01
30	6.84E-07	6.66E-07	6.75E-07	6.31E-02
35	3.79E-07	3.79E-07	3.79E-07	3.54E-02
40	2.08E-07	2.02E-07	2.05E-07	1.92E-02
45	1.12E-07	1.09E-07	1.11E-07	1.03E-02
50	6.07E-08	5.91E-08	5.99E-08	5.60E-03

Appendix C

Table C1: The detected photon flux from X-rays source with 60keV energy beyond wood shield for respective thicknesses and the transmission.

thickness(cm)	Flux at point 1 (photons/cm^2)	Flux at point 2 (photons/cm^2)	Average (photon/cm^2)	transmission
5	6.85E-06	6.42E-06	6.63E-06	6.44E-01
10	4.32E-06	4.05E-06	4.18E-06	4.06E-01
15	2.67E-06	2.51E-06	2.59E-06	2.52E-01
20	1.63E-06	1.53E-06	1.58E-06	1.53E-01
25	9.78E-07	9.17E-07	9.48E-07	9.20E-02
30	5.80E-07	5.45E-07	5.62E-07	5.46E-02
35	2.92E-07	2.77E-07	2.85E-07	2.76E-02
40	1.98E-07	1.86E-07	1.92E-07	1.87E-02
45	1.14E-07	1.08E-07	1.11E-07	1.08E-02
50	6.55E-08	6.22E-08	6.39E-08	6.20E-03

Table C2: The detected photon flux from X-rays source with 120keV energy beyond wood shield for respective thicknesses and the transmission.

thickness(cm)	Flux at point 1 (photons/cm^2)	Flux at point 2 (photons/cm^2)	Average flux (photons/cm^2)	transmission
5	7.59E-06	7.14E-06	7.36E-06	6.88E-01
10	5.33E-06	5.02E-06	5.18E-06	4.84E-01
15	3.73E-06	3.52E-06	3.62E-06	3.39E-01
20	2.58E-06	2.44E-06	2.51E-06	2.35E-01
25	1.77E-06	1.67E-06	1.72E-06	1.61E-01
30	1.20E-06	1.14E-06	1.17E-06	1.09E-01
35	6.88E-07	6.58E-07	6.73E-07	6.29E-02
40	5.33E-07	5.08E-07	5.21E-07	4.86E-02
45	3.52E-07	3.36E-07	3.44E-07	3.22E-02
50	2.21E-07	2.31E-07	2.26E-07	2.12E-02

Table C3: The detected photon flux from X-rays source with 300keV energy beyond wood shield for respective thicknesses and the transmission.

thickness(cm)	Flux at point 1 (Photons/cm^2)	Flux at point 2 (photons/cm^2)	Average flux (photons/cm^2)	Transmission
5	8.26E-06	7.80E-06	8.03E-06	7.50E-01
10	6.26E-06	5.93E-06	6.09E-06	5.70E-01
15	4.74E-06	4.50E-06	4.62E-06	4.32E-01
20	3.56E-06	3.39E-06	3.48E-06	3.25E-01
25	2.66E-06	2.54E-06	2.60E-06	2.43E-01
30	1.97E-06	1.88E-06	1.93E-06	1.80E-01
35	1.25E-06	1.21E-06	1.23E-06	1.15E-01
40	1.06E-06	1.01E-06	1.04E-06	9.67E-02
45	7.67E-07	7.38E-07	7.52E-07	7.03E-02
50	5.34E-07	5.54E-07	5.44E-07	5.09E-02

Table C4: The detected photon flux from X-rays source with 60keV energy beyond clay shield for respective thicknesses and the transmission.

Thickness(cm)	Flux at point 1 (photons/cm^2)	Flux at point 2 (photons/cm^2)	Average flux (photons/cm^2)	Transmission
1	6.56E-06	6.10E-06	6.33E-06	6.14E-01
2	3.86E-06	3.54E-06	3.70E-06	3.59E-01
5	6.33E-07	7.12E-07	6.73E-07	6.53E-02

10	3.70E-08	3.14E-08	3.42E-08	3.32E-03
15	1.80E-09	1.52E-09	1.66E-09	1.61E-04
20	9.20E-11	8.85E-11	9.02E-11	8.76E-06
25	6.07E-12	4.78E-12	5.42E-12	5.27E-07
30	1.27E-13	9.74E-14	1.12E-13	1.09E-08
35	3.28E-15	2.33E-15	2.81E-15	2.73E-10
40	8.82E-17	6.04E-17	7.43E-17	7.21E-12

Table C5: The detected photon flux from X-rays source with 120keV energy beyond clay shield for respective thicknesses and the transmission.

Thickness(cm)	Flux at point 1 (photons/cm^2)	Flux at point 2 (photons/cm^2)	Average flux (photons/cm^2)	Transmission
1	8.81E-06	8.25E-06	8.53E-06	7.97E-01
2	7.10E-06	6.62E-06	6.86E-06	6.41E-01
5	3.53E-06	3.26E-06	3.40E-06	3.18E-01
10	9.34E-07	8.53E-07	8.94E-07	8.35E-02
15	2.21E-07	1.99E-07	2.10E-07	1.96E-02
20	4.96E-08	4.41E-08	4.69E-08	4.38E-03
25	1.07E-08	9.48E-09	1.01E-08	9.43E-04
30	2.23E-09	1.93E-09	2.08E-09	1.94E-04
35	4.08E-10	4.70E-10	4.39E-10	4.10E-05
40	1.00E-10	8.32E-11	9.18E-11	8.58E-06

Table C6: The detected photon flux from X-rays source with 300keV energy beyond clay shield for respective thicknesses and the transmission.

Thickness(cm)	pt A	Pt b	average	300KeV transmission
1	9.60E-06	9.02E-06	9.31E-06	8.70E-01
2	8.47E-06	7.95E-06	8.21E-06	7.67E-01
5	5.76E-06	5.37E-06	5.57E-06	5.20E-01
10	2.70E-06	2.51E-06	2.60E-06	2.43E-01
15	1.14E-06	1.05E-06	1.09E-06	1.02E-01
20	4.12E-07	4.47E-07	4.29E-07	4.01E-02
25	1.70E-07	1.56E-07	1.63E-07	1.52E-02
30	6.22E-08	5.70E-08	5.96E-08	5.57E-03
35	2.24E-08	2.04E-08	2.14E-08	2.00E-03
40	7.91E-09	7.28E-09	7.60E-09	7.10E-04

Table C7: The detected photon flux from X-rays source with 60keV energy beyond sandstone shield for respective thicknesses and the transmission.

Thickness(cm)	Flux at point 1(photons/cm^2)	Flux at point 2 (photons/cm^2)	Average Flux (photons/cm^2)	Transmission
1	6.70E-06	6.23E-06	6.47E-06	6.28E-01
2	4.04E-06	3.71E-06	3.87E-06	3.76E-01
5	7.90E-07	7.05E-07	7.48E-07	7.26E-02
10	4.42E-08	3.81E-08	4.12E-08	4.00E-03
15	2.27E-09	1.91E-09	2.09E-09	2.03E-04
20	1.11E-10	8.67E-11	9.89E-11	9.61E-06
25	5.77E-12	7.03E-12	6.40E-12	6.21E-07
30	3.73E-13	3.45E-13	3.59E-13	3.49E-08

Table C8: The detected photon flux from X-rays source with 120keV energy beyond sandstone shield for respective thicknesses and the transmission.

Thickness(cm)	Flux at point 1 (photons/cm^2)	Flux at point 2 (photons/cm^2)	Average flux	Transmission
1	8.74E-06	8.18E-06	8.46E-06	7.91E-01
2	7.01E-06	6.54E-06	6.77E-06	6.33E-01
5	3.42E-06	3.15E-06	3.28E-06	3.07E-01
10	7.74E-07	8.52E-07	8.13E-07	7.60E-02
15	1.87E-07	1.69E-07	1.78E-07	1.66E-02
20	3.92E-08	3.47E-08	3.69E-08	3.45E-03
25	7.76E-09	6.91E-09	7.34E-09	6.86E-04
30	1.29E-09	1.47E-09	1.38E-09	1.29E-04

Table C9: The detected photon flux from X-rays source with 300keV energy beyond sandstone shield for respective thicknesses and the transmission.

Thickness(cm)	Flux at point 1 (photons/cm^2)	Flux at point 2 (photons/cm^2)	Average (photons/cm^2)	Transmission
1	9.54E-06	8.97E-06	9.25E-06	8.65E-01
2	8.38E-06	7.86E-06	8.12E-06	7.59E-01
5	5.61E-06	5.23E-06	5.42E-06	5.06E-01
10	2.52E-06	2.33E-06	2.43E-06	2.27E-01
15	1.00E-06	9.24E-07	9.64E-07	9.01E-02
20	3.74E-07	3.43E-07	3.58E-07	3.35E-02
25	1.33E-07	1.22E-07	1.27E-07	1.19E-02
30	4.58E-08	4.20E-08	4.39E-08	4.10E-03
35	1.54E-08	1.40E-08	1.47E-08	1.37E-03

Appendix D Example of MCNP file Used in this study

Below is the copy of an MNCP input file used to compute the photon flux beyond wood shield from cobalt 60 gamma source and its transmission through 50 cm thick wood. This file should be considered as a typical example of the type of layout used in this study which was modified with fairly simple alterations to compute other results presented in this work.

```
c MCNP input for wood shielding effectiveness computation
c cell cards
1 1 -0.64000 1 -2 3 -4 5 -6              imp:p=1   $ shield
2 2 -0.001225 7 -8 9 -10 11 -12          imp:p=2   $ source region
3 1 -0.64000 13 -20 15 -16 17 -18        imp:p=3
4 1 -0.64000 20 -21 15 -16 17 -18        imp:p=4
5 1 -0.64000 21 -22 15 -16 17 -18        imp:p=5
6 1 -0.64000 22 -23 15 -16 17 -18        imp:p=6
7 1 -0.64000 23 -24 15 -16 17 -18        imp:p=7
8 1 -0.64000 24 -25 15 -16 17 -18        imp:p=8
9 1 -0.64000 25 -26 15 -16 17 -18        imp:p=9
10 1 -0.64000 26 -27 15 -16 17 -18       imp:p=10
```

11 2 -0.001225 27 -14 15 -16 17 -18 imp:p=5 $ behind the shield, detector region

c 5 2 -0.001225 19 -14 15 -16 17 -18 imp:p=5 $ detector volume

12 0 #1 #2 #3 #4 #5 #6 #7 #8 #9 #10 #11 imp:p=0 $outside world

c surface cards

1 px 0

2 px 10

3 py 0

4 py 50

5 pz 0

6 pz 50

7 px -100

8 px 0

9 py 0

10 py 50

11 pz 0

12 pz 50

13 px 10

14 px 80

15 py 0

16 py 50

17 pz 0

18 pz 50

c 19 px 29.999

20 px 15

21 px 20

22 px 25

23 px 30

24 px 35

25 px 40

26 px 45

27 px 50

mode p

c material card

m1 1000 -0.059642 $ southern pine wood

```
     6000  -0.497018
     7000  -0.004970
     8000  -0.427435
     12000 -0.001988
     16000 -0.004970
     19000 -0.001988
     20000 -0.001988
m2   7000 -0.755267 $ AIR
     8000 -0.231781
     18000 -0.012827
     6000 -0.000124
c source
sdef pos=-50 5 5 CEL=2 NRM=+1 VEC=1 0 0 PAR=2 ERG=D1
SI1 L 1.1732 1.3325
SP1 D 1.0 1.0
c tally cards
f5:p 80 25 25 1 80 30 30 1
c DE 1.0 1.4
```

c DF 1.98E-6 2.51E-6

nps 100000000

Appendix E Sample calculation for net Cost-benefit B

Below is the procedure to perform cost-Benefit analysis for wood which should be considered as the sample procedure which can be modified simply by altering parameters to perform analysis for other materials whose results are presented in this work.

First calculating number of HVLs required to reduce 0.034 Sv/year to 1 mSv/year:

$$\frac{10^{-3}Sv/year}{0.034Sv/year} = \frac{1}{2^n}$$

$$n = \frac{ln34}{ln2} = 5.1$$

Thus n = 5.1 HVLs

For wood HVLs was found to 18 cm for cobalt 60, thus n = 5.1 x 18 cm = 91 cm, this thickness has a buildup factor of 3.8 when extrapolating the curve of thickness vs buildup factors for wood.

Thus, r was calculated as follows:

$$\mathrm{r} = \frac{1}{91\ cm}\left(\ln\left(\frac{\frac{0.034Sv}{year}x3.8}{\frac{1mSv}{year}}\right) = 5.3\ m^{-1}\right.$$

computing the dose reduction factor using equation (17);

$$e^{-rw} = \frac{\$50\ m^{-3} x\ 6\ m^2 man^{-1}}{\$100(manSv)^{-1} x\ 5.3m^{-1} x\ 0.034Svy^{-1} x\ 20\ y} = 0.83$$

Then computing the cost X(w) of installation using equation (16):

$$X(w) = \$50m^{-3} x\ 9m\ x\ 9m\ x\ 0.9m + \$750 = \$4395$$

The cost of detriment Y(w) according to equation was calculated using equation (14) as follows:

$$Y(w) = \$1000(manSv)^{-1}m^{-2}\ x\ 0.034Svy^{-1}\ x\ 20y\ x\ 1\ x\ 6m^2man^{-1} = \$338.64$$

The computed values of X and Y were used to compute the benefit B of using wood instead of lead assumed to cost $10000 using equation (13):

$$B = \$10000 - (\$1000 + 4395 + 338.64) = \$4266.36$$